Nonlinear hypocentre determination

Petr Bulant, Václav Bucha, Luděk Klimeš

Charles University in Prague, Faculty of Mathematics and Physics, Department of Geophysics

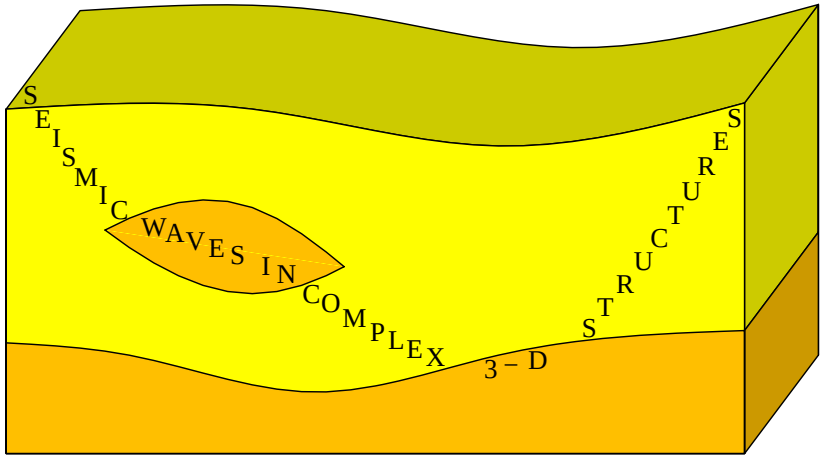

http://sw3d.cz

Seminar on seismology, Praha, 27.11.2015

Hypocentre determination

Hypocentre determination means calculation of coordinates of the hypocentre and of the hypocentral time, i.e. 4 unknown quantities.

We calculate them from measured arrival times, and thus, theoretically, 4 arrival times could be sufficient for hypocentre determination (assuming perfect measurement of the arrival times, perfect knowledge of the structure and perfect modelling of the theoretical travel times).

This presentation is devoted to possibilities how to make use of the surplus (above the 4 essentially needed) arrivals in the standard situation, when neither arrival time measurement, nor the knowledge of the structure and theoretical travel times are perfect.

Hypocentre determination

Hypocentre determination means calculation of coordinates of the hypocentre and of the hypocentral time of a seismic event. We calculate them from a seismic recording of the event.

Hypocentre determination

Usually, we calculate the hypocentre location from the measured arrival times of seismic body waves (P-waves and/or S-waves).

Hypocentre determination

Nevertheless, the measured P-wave and S-wave arrival times are not sufficient for hypocentre location.

Hypocentre determination

We need to know also the velocity model of the structure in which we are able to calculate the theoretical travel times.

Hypocentre determination

We need to know also the velocity model of the structure in which we are able to calculate the theoretical travel times. Then we can calculate the hypocentre location as a space-time point with minimum difference between the theoretical travel times and measured arrival times.

Hypocentre determination

But, usually, we are interested not only in the hypocentre location (as a space-time point with minimum difference between the theoretical travel times and measured arrival times), but also in the uncertainty of the location.

Hypocentre determination

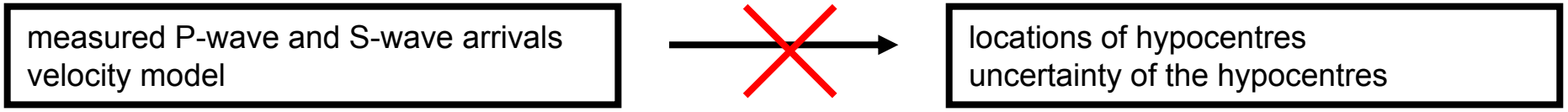

Then the arrival times and velocity model are not sufficient input for the location, ….

Hypocentre determination

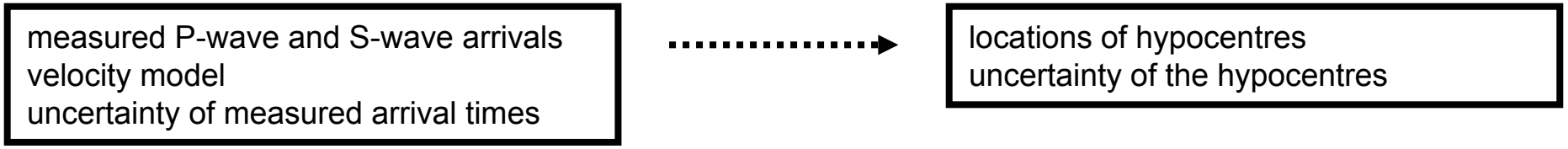

Then the arrival times and velocity model are not sufficient input for the location, and we need to add the uncertainty of the measured arrival times, ….

Hypocentre determination

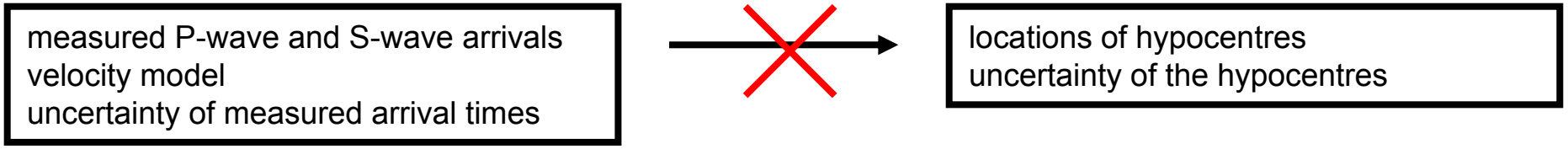

The uncertainty of the measured arrival times can technically produce some uncertainty of the hypocentres. But, using only the uncertainty of arrival times in fact means assuming perfect knowledge of the structure and perfect modelling, which is usually not the case.

Hypocentre determination

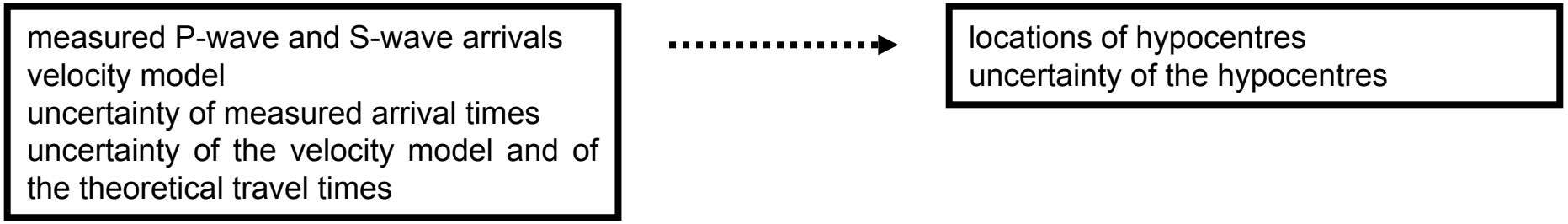

Thus, the arrival times and velocity model are not sufficient input for the location, and we need to add the uncertainty of the measured arrival times, and the uncertainty of the velocity model, and the uncertainty caused by the errors of the theoretical travel times.

Hypocentre determination

Thus, the arrival times and velocity model are not sufficient input for the location, and we need to add the uncertainty of the measured arrival times, and the uncertainty of the velocity model, and the uncertainty caused by the errors of the theoretical travel times. Then we can obtain the hypocentre location as not only a single space-time point, but as a probability function which describes the uncertainty of the location.

Hypocentre determination

measured P-wave and S-wave arrivals
velocity model
uncertainty of measured arrival times
uncertainty of the model and travel times

locations of hypocentres
uncertainty of the hypocentres

Hypocentre determination

measured P-wave and S-wave arrivals
velocity model
uncertainty of measured arrival times
uncertainty of the model and travel times

locations of hypocentres
uncertainty of the hypocentres

The method

Hypocentre determination

measured P-wave and S-wave arrivals
velocity model
uncertainty of measured arrival times
uncertainty of the model and travel times

locations of hypocentres
uncertainty of the hypocentres

Tarantola & Valette (1982): nonlinear hypocentre determination consisting in direct evaluation of the nonnormalized 3-D marginal a posteriori density function which describes the relative probability of the seismic hypocentre, discretized at the gridpoints of a sufficiently dense 3-D spatial grid of points.

We describe the uncertainty of the velocity model by the model covariance function, which is projected onto the uncertainty of the hypocentral position through the geometrical covariances of theoretical travel times calculated in the velocity model (Klimeš 2002a, 2008).

Hypocentre determination

measured P-wave and S-wave arrivals
velocity model
uncertainty of measured arrival times
uncertainty of the model and travel times

→

locations of hypocentres
uncertainty of the hypocentres

Tarantola & Valette (1982): nonlinear hypocentre determination consisting in direct evaluation of the nonnormalized 3-D marginal a posteriori density function which describes the relative probability of the seismic hypocentre, discretized at the gridpoints of a sufficiently dense 3-D spatial grid of points.

We describe the uncertainty of the velocity model by the model covariance function, which is projected onto the uncertainty of the hypocentral position through the geometrical covariances of theoretical travel times calculated in the velocity model (Klimeš 2002a, 2008).

uncertainty of the velocity model
described by model covariance function

geometrical
travel-time
covariance matrix
→

nonnormalized 3-D marginal a posteriori density function

Hypocentre determination

measured P-wave and S-wave arrivals
velocity model
uncertainty of measured arrival times
uncertainty of the model and travel times

→

locations of hypocentres
uncertainty of the hypocentres

Tarantola & Valette (1982): nonlinear hypocentre determination consisting in direct evaluation of the nonnormalized 3-D marginal a posteriori density function which describes the relative probability of the seismic hypocentre, discretized at the gridpoints of a sufficiently dense 3-D spatial grid of points.

We describe the uncertainty of the velocity model by the model covariance function, which is projected onto the uncertainty of the hypocentral position through the geometrical covariances of theoretical travel times calculated in the velocity model (Klimeš 2002a, 2008).

uncertainty of the velocity model
described by model covariance function

→ geometrical travel-time covariance matrix

nonnormalized 3-D marginal a posteriori density function

↓

minimum arrival-time residuals
(arrival-time misfit)

Hypocentre determination

measured P-wave and S-wave arrivals
velocity model
uncertainty of measured arrival times
uncertainty of the model and travel times

→

locations of hypocentres
uncertainty of the hypocentres

Tarantola & Valette (1982): nonlinear hypocentre determination consisting in direct evaluation of the nonnormalized 3-D marginal a posteriori density function which describes the relative probability of the seismic hypocentre, discretized at the gridpoints of a sufficiently dense 3-D spatial grid of points.

We describe the uncertainty of the velocity model by the model covariance function, which is projected onto the uncertainty of the hypocentral position through the geometrical covariances of theoretical travel times calculated in the velocity model (Klimeš 2002a, 2008).

uncertainty of the velocity model described by model covariance function

→ geometrical travel-time covariance matrix →

nonnormalized 3-D marginal a posteriori density function

↓

minimum arrival-time residuals (arrival-time misfit)

↓

estimation of the uncertainty of the velocity model

The minimum arrival-time residuals carry information pertinent to the accuracy of the velocity model (Klimeš 1996)

Hypocentre determination

measured P-wave and S-wave arrivals
velocity model
uncertainty of measured arrival times
uncertainty of the model and travel times

→

locations of hypocentres
uncertainty of the hypocentres

Tarantola & Valette (1982): nonlinear hypocentre determination consisting in direct evaluation of the nonnormalized 3-D marginal a posteriori density function which describes the relative probability of the seismic hypocentre, discretized at the gridpoints of a sufficiently dense 3-D spatial grid of points.

We describe the uncertainty of the velocity model by the model covariance function, which is projected onto the uncertainty of the hypocentral position through the geometrical covariances of theoretical travel times calculated in the velocity model (Klimeš 2002a, 2008).

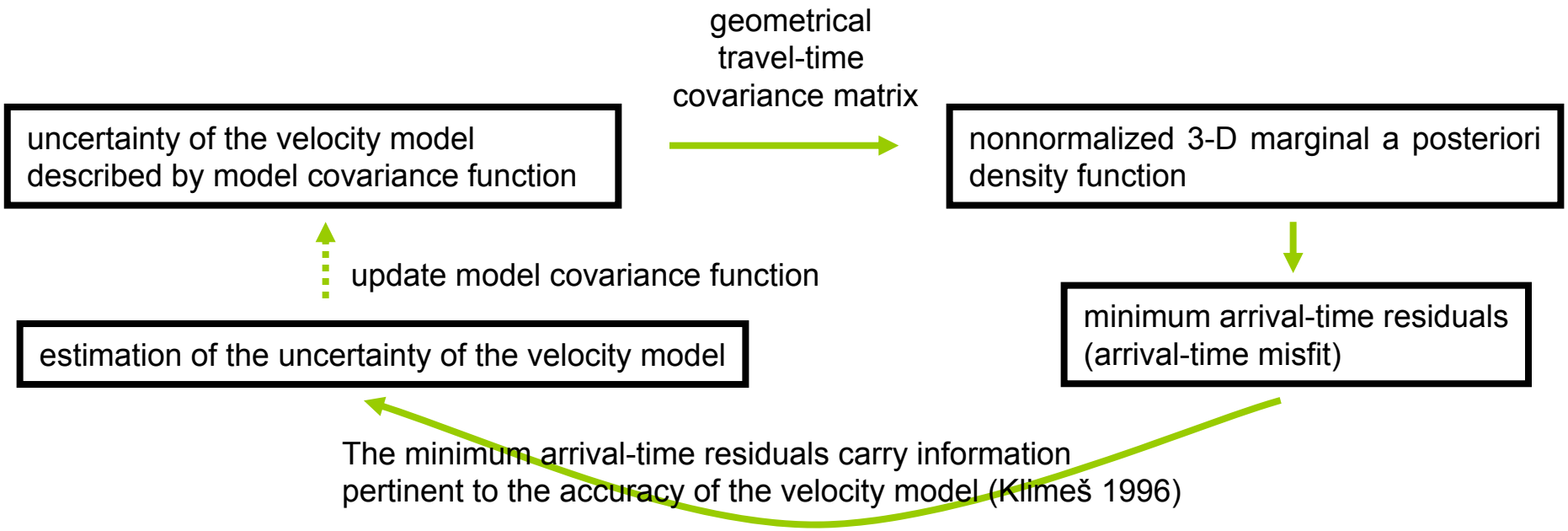

Hypocentre determination

measured P-wave and S-wave arrivals
velocity model
uncertainty of measured arrival times
uncertainty of the model and travel times

→

locations of hypocentres
uncertainty of the hypocentres
uncertainty of the velocity model

Tarantola & Valette (1982): nonlinear hypocentre determination consisting in direct evaluation of the nonnormalized 3-D marginal a posteriori density function which describes the relative probability of the seismic hypocentre, discretized at the gridpoints of a sufficiently dense 3-D spatial grid of points.

We describe the uncertainty of the velocity model by the model covariance function, which is projected onto the uncertainty of the hypocentral position through the geometrical covariances of theoretical travel times calculated in the velocity model (Klimeš 2002a, 2008).

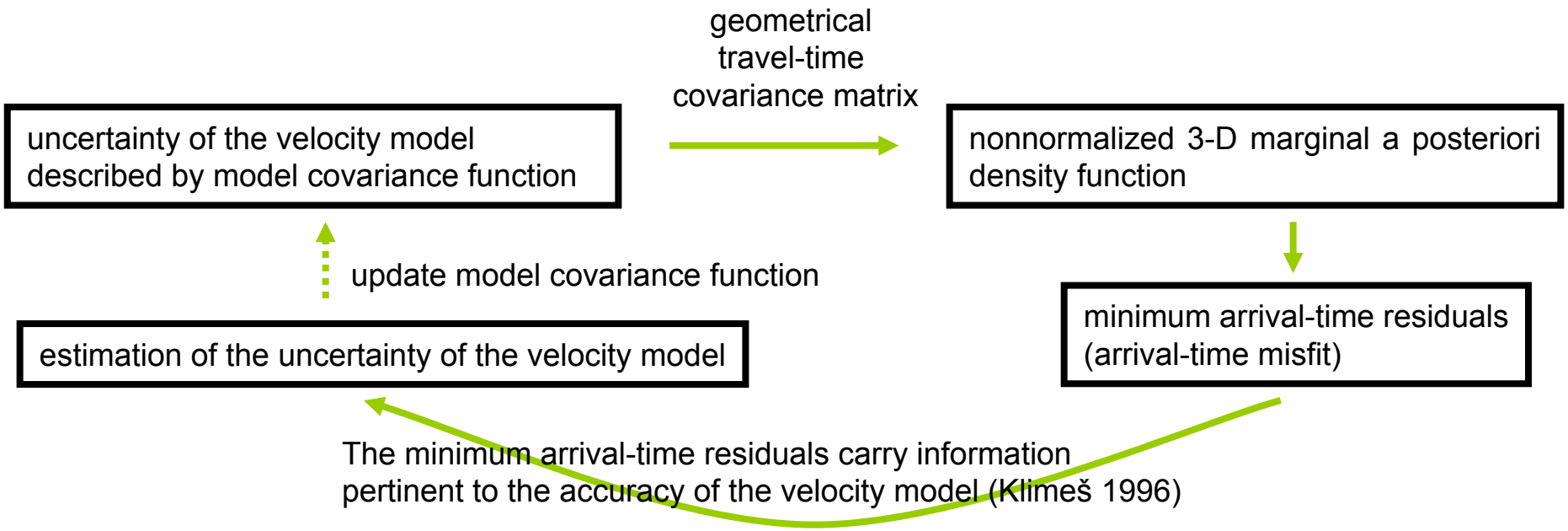

Hypocentre determination

measured P-wave and S-wave arrivals
velocity model
uncertainty of measured arrival times
uncertainty of travel-time computing

→

locations of hypocentres
uncertainty of the hypocentres
uncertainty of the velocity model

Tarantola & Valette (1982): nonlinear hypocentre determination consisting in direct evaluation of the nonnormalized 3-D marginal a posteriori density function which describes the relative probability of the seismic hypocentre, discretized at the gridpoints of a sufficiently dense 3-D spatial grid of points.

We describe the uncertainty of the velocity model by the model covariance function, which is projected onto the uncertainty of the hypocentral position through the geometrical covariances of theoretical travel times calculated in the velocity model (Klimeš 2002a, 2008).

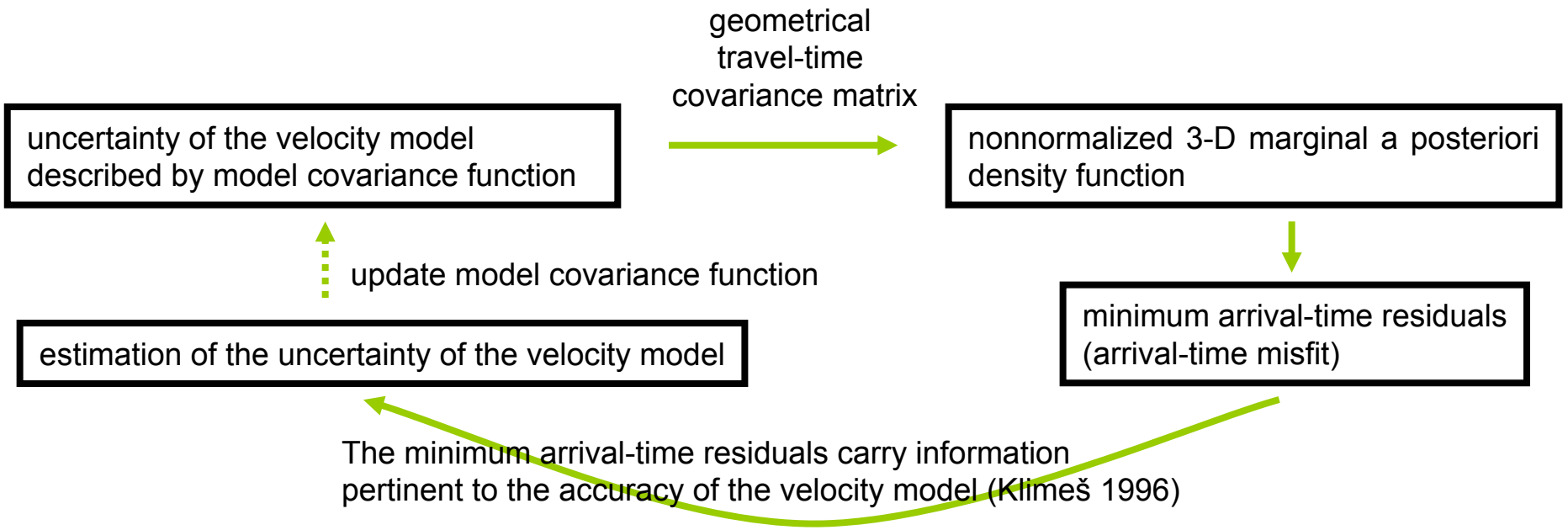

Notes on numerical implementation of the algorithm

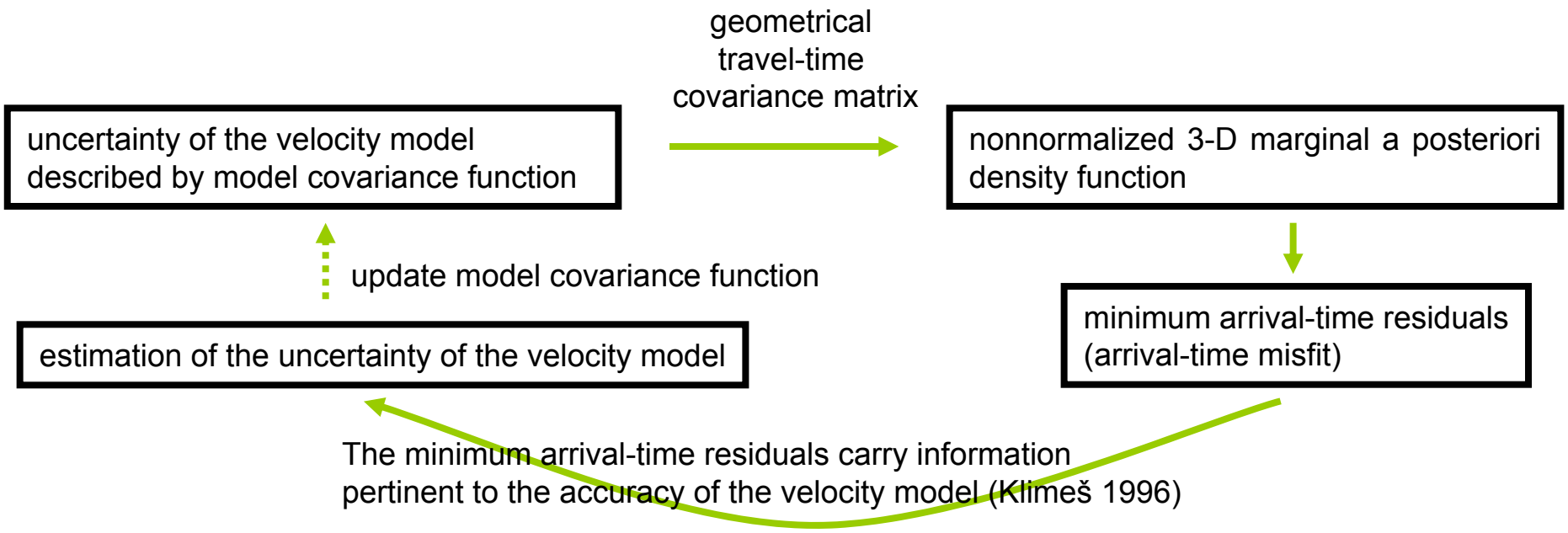

Notes on numerical implementation of the algorithm

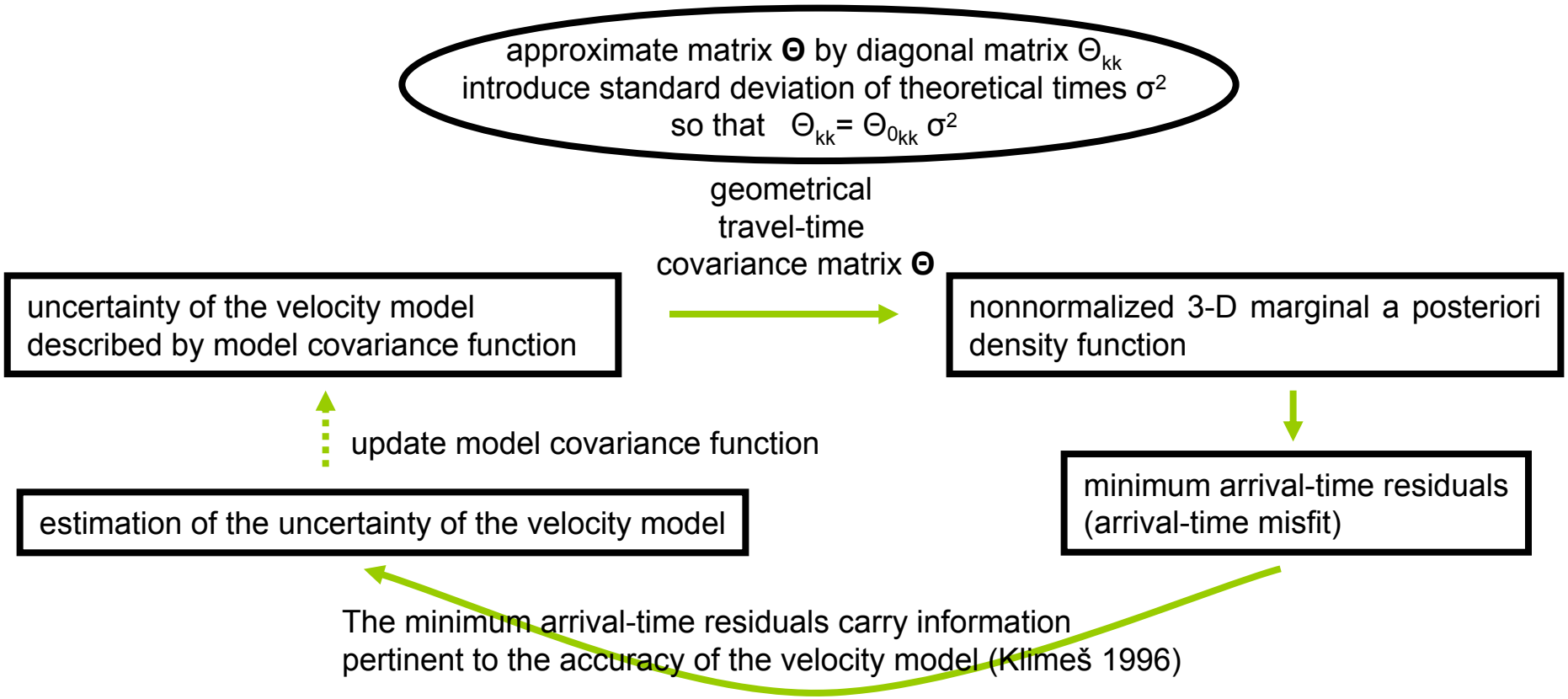

Notes on numerical implementation of the algorithm

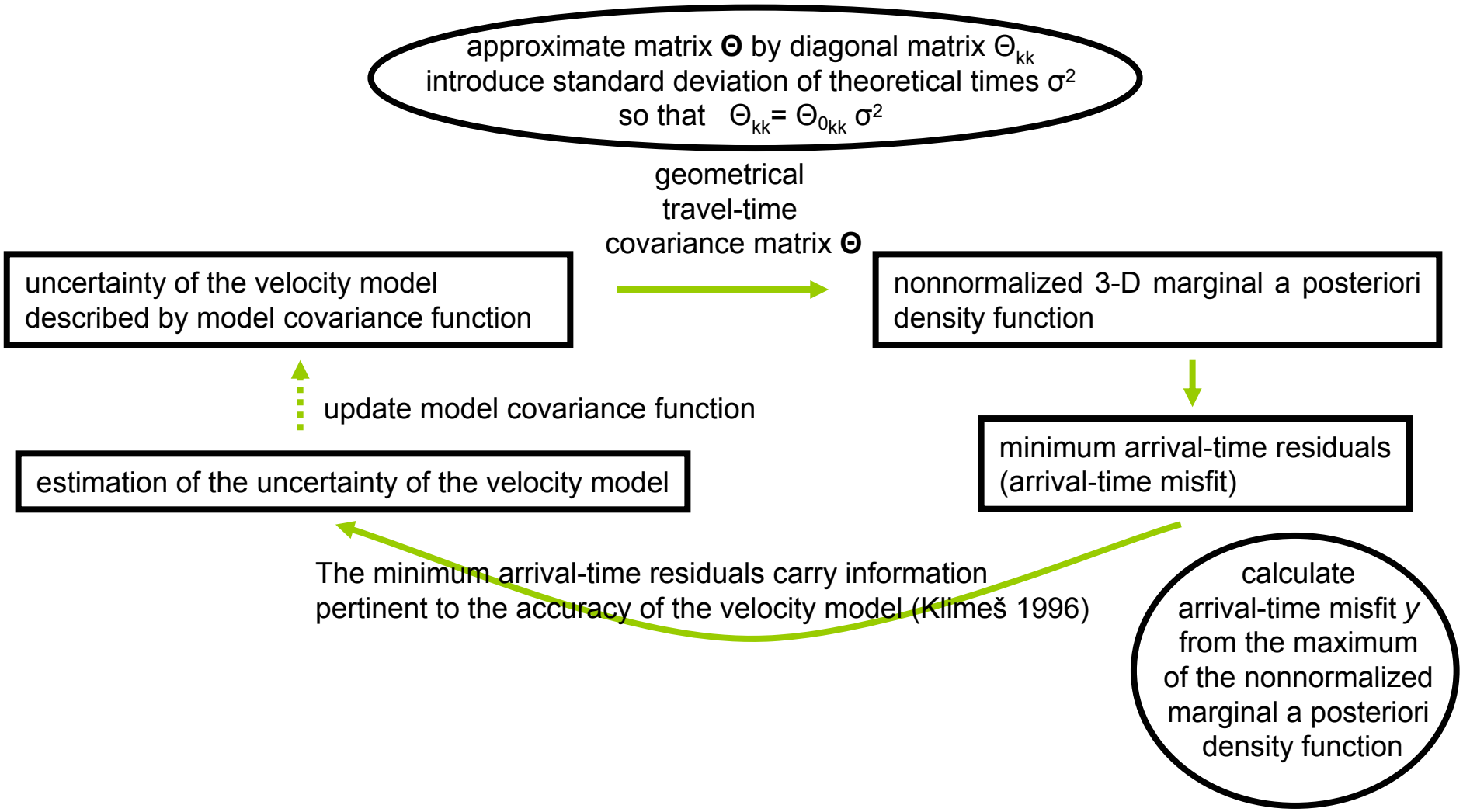

Notes on numerical implementation of the algorithm

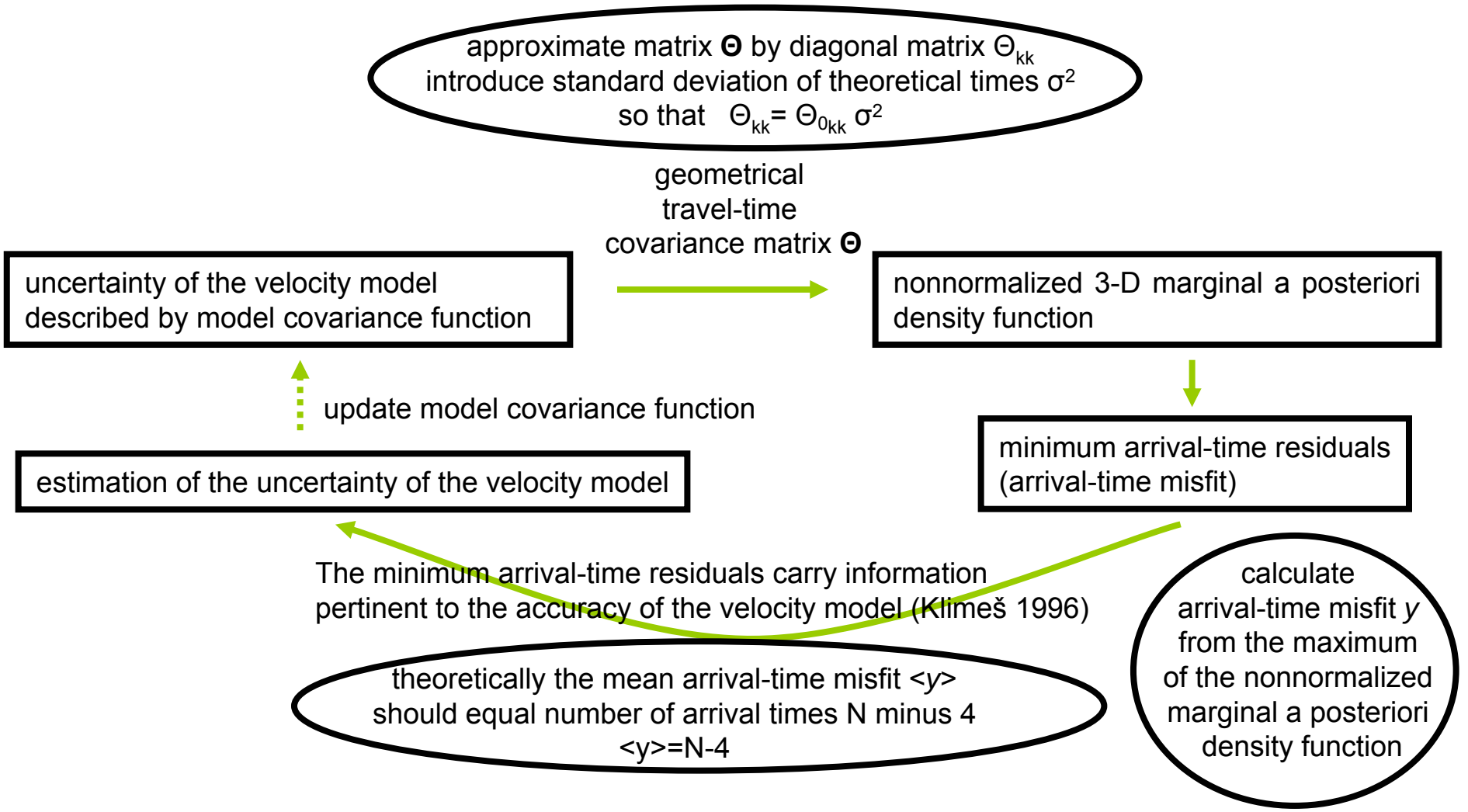

Numerical examples

2 numerical examples:

1) 4 local natural earthquakes in Western Bohemia

2) Microseismic monitoring of 33 natural events

Numerical example 1

- 4 local natural events in Western Bohemia
- 10 stations (event no 4 was registered only on 6 stations)
- P-wave arrival times only
- smooth 3-D velocity model of Western Bohemia (Klimes 1995)
- standard deviations of theoretical travel times and the Hurst exponent obtained from refraction measurements (Klimes 2002b)

Numerical example 1

approximate matrix **Θ** by diagonal matrix Θ_{kk}
introduce standard deviation of theoretical times σ^2
so that $\Theta_{kk} = \Theta_{0kk}\,\sigma^2$

geometrical
travel-time
covariance matrix **Θ**

uncertainty of the velocity model
described by model covariance function

→

nonnormalized 3-D marginal a posteriori
density function

↓

minimum arrival-time residuals
(arrival-time misfit *y*)

The minimum arrival-time residuals carry information
pertinent to the accuracy of the velocity model (Klimeš 1996)

theoretically the mean arrival-time misfit $\langle y \rangle$
should equal number of arrival times N minus 4
$\langle y \rangle = N-4$

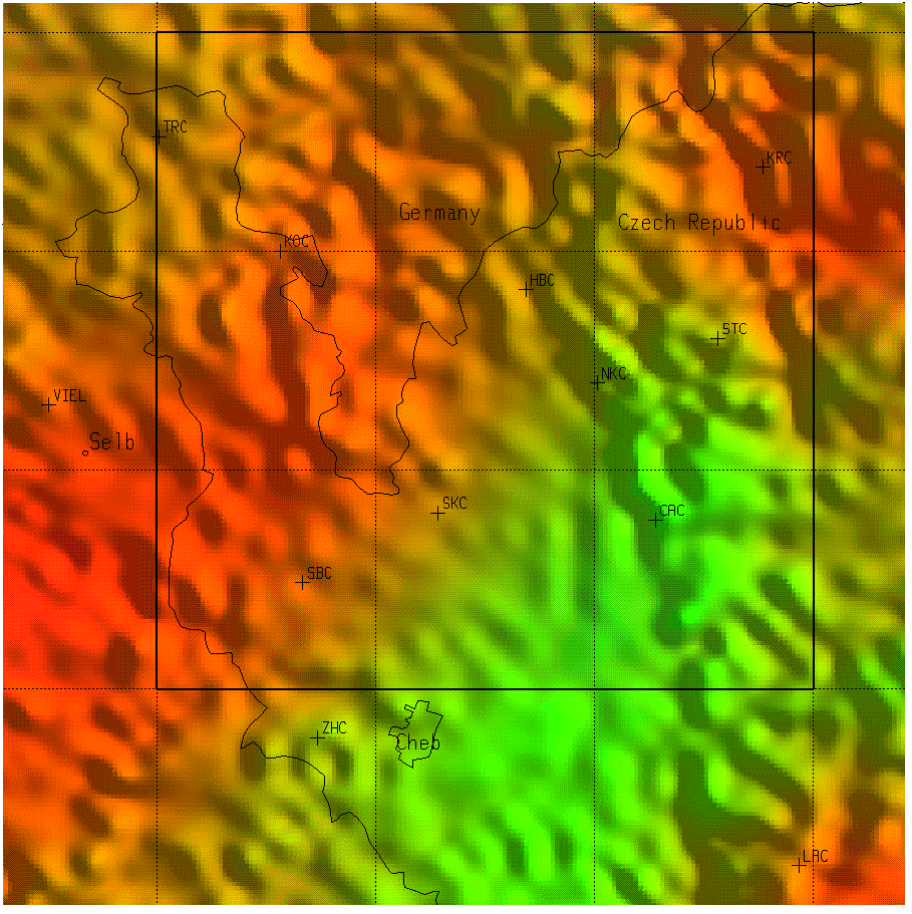

Part of the Western Bohemia a priori velocity model with the receivers and surface P wave velocities (the shadows are caused by the topography). Values of the velocity increase from **green** to **red** colour. The thick line rectangle limits the location grid, 30 × 30 km, depth is 17 km. The grid step is 0.5 km in all three directions. Receivers HBC and STC are not considered.

Measured data

- **The hypocentre determination code is tested by determining hypocentres of four local earthquakes recorded on January 1997 by the WEBNET local seismic network and one receiver in Germany.**
- **Three tested local earthquakes were measured by 10 receivers and one event was recorded by 6 receivers.**

receiver	*event 1*	*event 2*	*event 3*	*event 4*
CAC–Částkov	30.168	45.100	59.812	21.292
KOC–Kopaniny	31.316	46.228	60.972	22.788
KRC–Kraslice	30.856	45.804	60.484	22.292
LAC–Lazy	32.720	47.656	62.340	
NKC–Nový Kostel	29.856	44.748	59.512	21.060
SBC–Seeberg	31.472	46.372	61.108	22.672
SKC–Skalná	30.484	45.376	60.140	21.636
TRC–Trojmezí	32.432	47.352	62.072	
VIEL–Viel	32.672	47.584	62.312	
ZHC–Zelená Hora	32.132	47.036	61.768	

Hypocentres

- For each event, the maximum σ_{P3}^{max} of the nonnormalized 3–D marginal a posteriori density function which describes the relative probability of the seismic hypocentre, and arrival–time misfit y:

event	σ_{P3}^{max}	$\langle y \rangle = N-4$	*y*
1	0.569	6	1.126
2	0.686	6	0.754
3	0.605	6	1.007
4	0.908	2	0.193

- Arrival-time missfit *y* is considerably smaller than its estimated mean value $\langle y \rangle$.
- We observed much greater uncertainty of the hypocentral position of event 4 determined just from six P–wave arrival times.
- We observed that the location of the maximum value of the nonnormalized 3–D marginal a posteriori density function may considerably differ from the mean hypocentre location given by the nonnormalized 3–D marginal a posteriori density function.
- Moreover, the mean hypocentre location often considerably depends on the dimensions of the location grid.

Seismically active region of Western Bohemia. The thick line rectangle limits the location grid. Four approximately elliptical curves limit the regions where the probability density functions of the four epicentres exceed 10% of the respective maximum values.

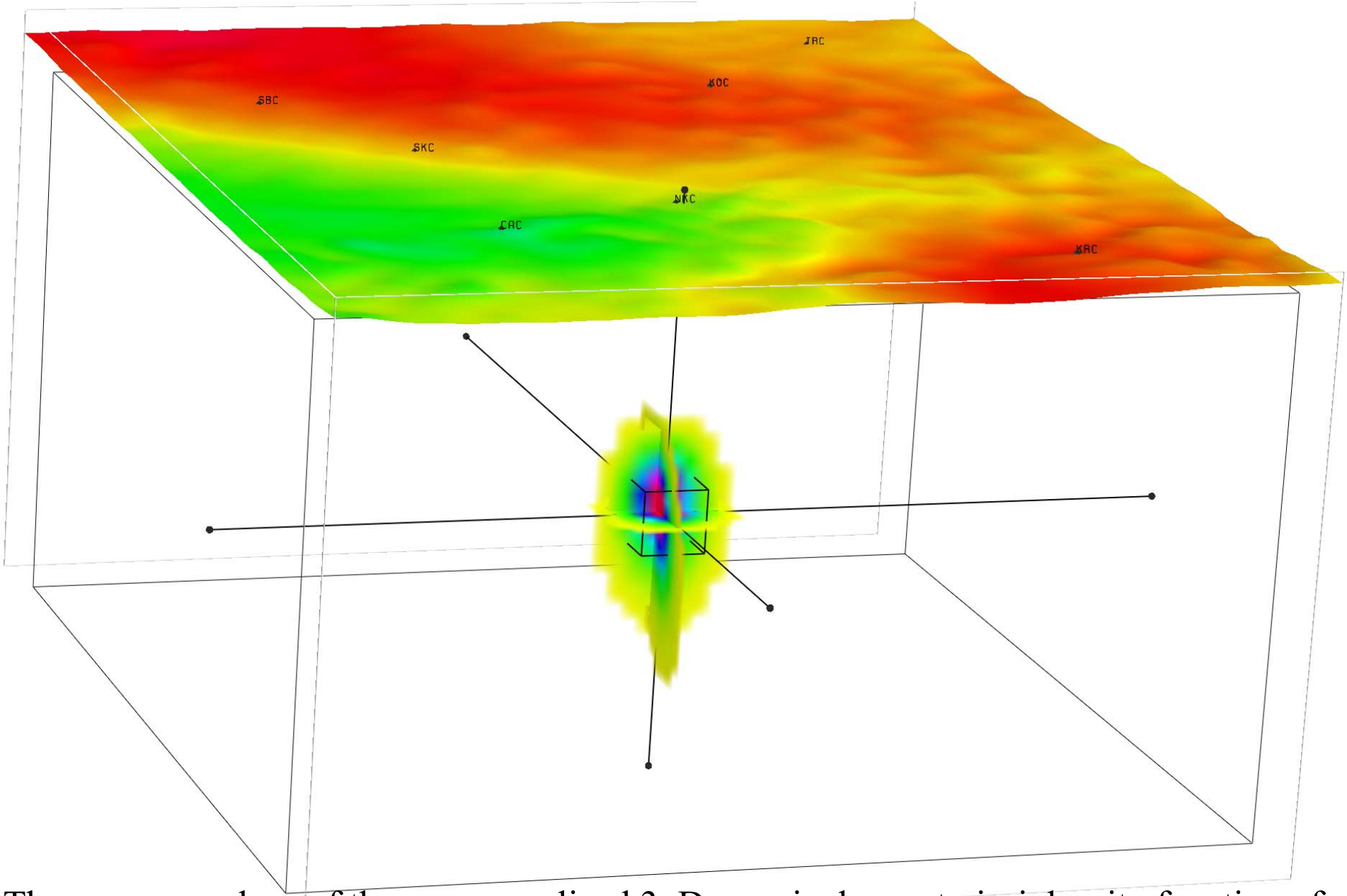

The nonzero values of the nonnormalized 3–D marginal a posteriori density function of **event 1** determined using 10 P–wave arrival times. The values range from yellow through green, cyan, blue and magenta to the maximum value displayed in red.

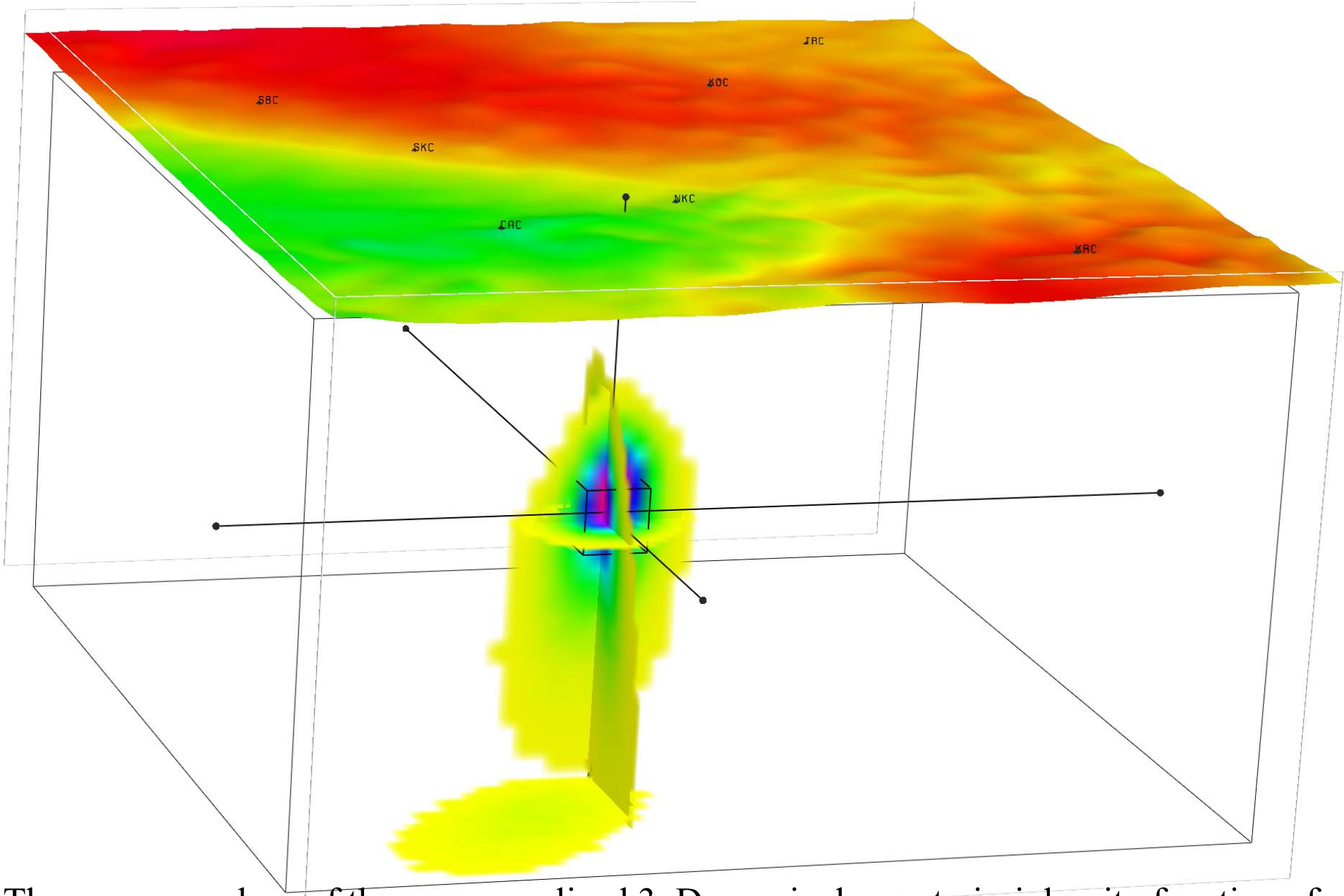

The nonzero values of the nonnormalized 3–D marginal a posteriori density function of **event 4** determined using 6 P–wave arrival times. The values range from yellow through green, cyan, blue and magenta to the maximum value displayed in red.

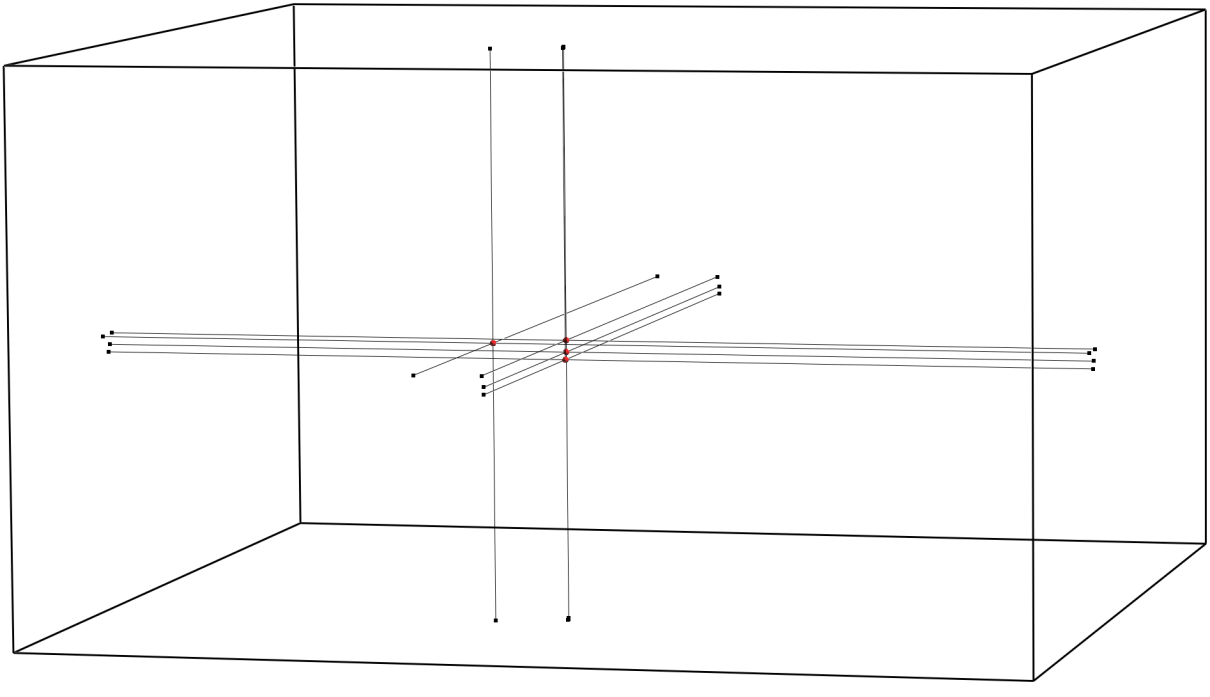

The locations of the centres of small cubes which are displayed as yardsticks (small **red** spheres), together with their projections onto the sides of the grid used for the nonlinear hypocentre determination. The displayed dimensions of the grid used for the nonlinear hypocentre determination are $30\,\mathrm{km}\times30\,\mathrm{km}\times17\,\mathrm{km}$.

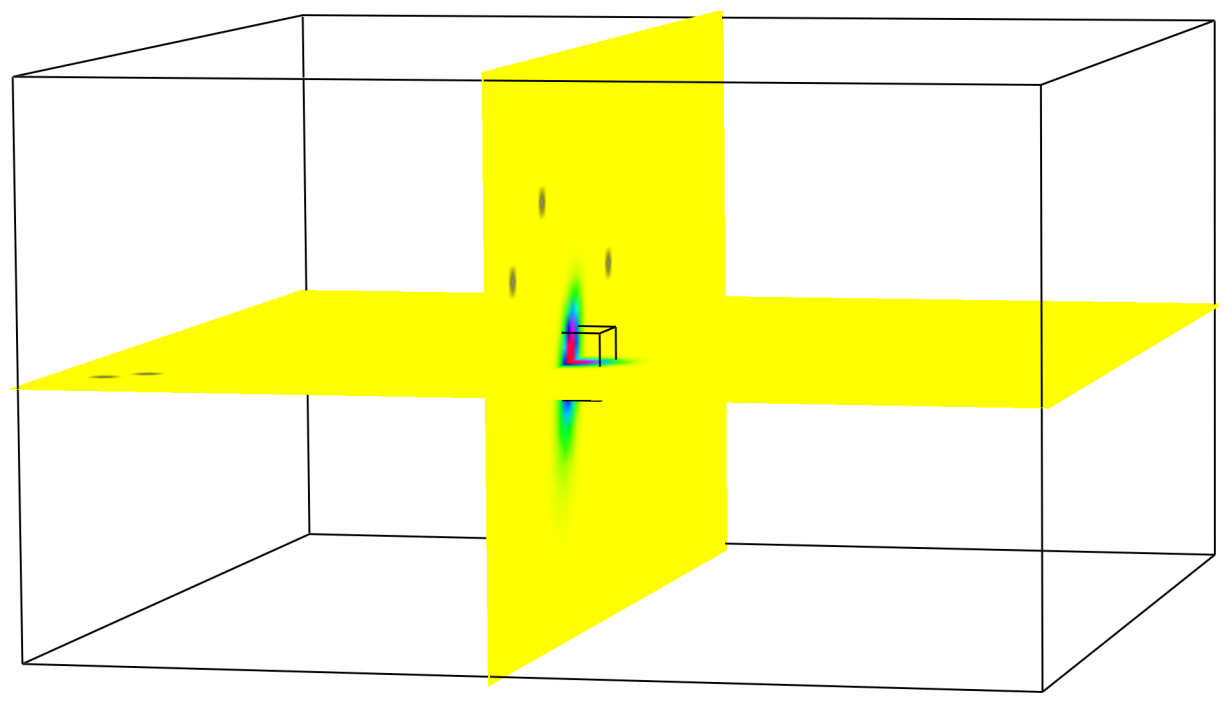

Nonnormalized 3–D marginal a posteriori density function of **event 1** determined using **10** P–wave arrival times. The zero values are displayed in **yellow**. The nonzero values range through **green**, **cyan**, **blue** and **magenta** to the maximum value displayed in **red**. The undefined values are displayed in **gray**, and denote the gridpoints at which at least one theoretical travel time is missing. The small cube has the sides of 2 km.

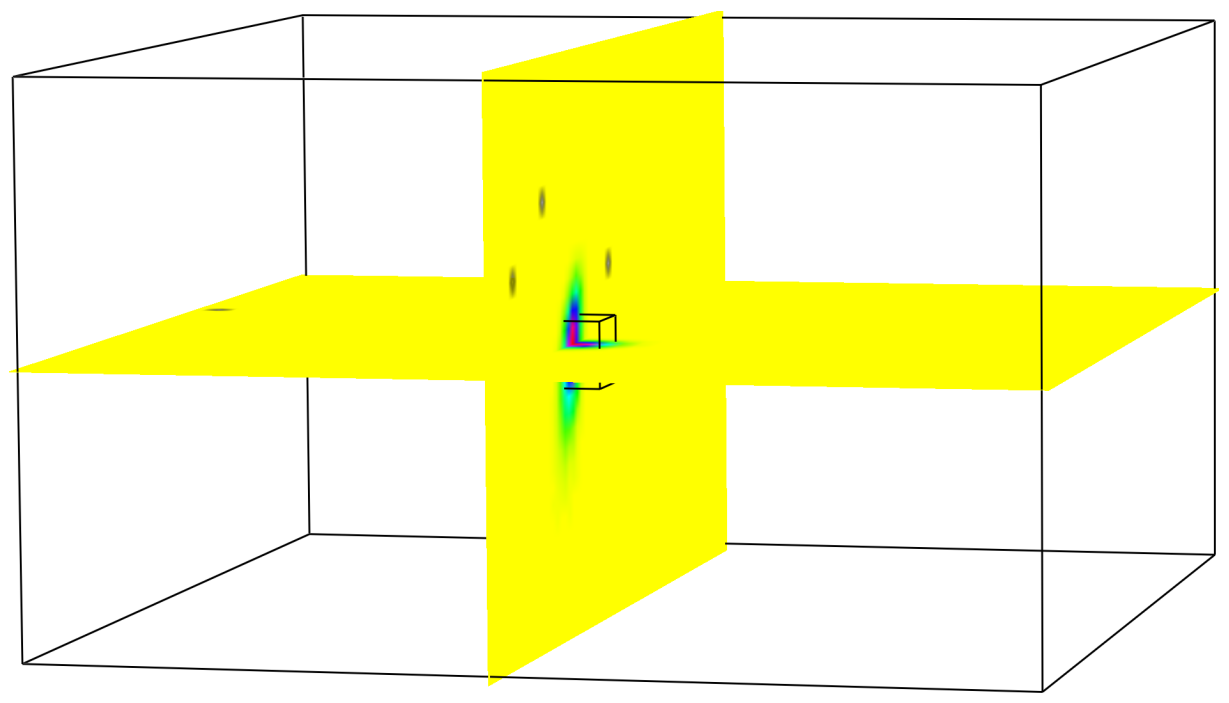

Nonnormalized 3–D marginal a posteriori density function of **event 2** determined using **10** P–wave arrival times. The zero values are displayed in **yellow**. The nonzero values range through **green**, **cyan**, **blue** and **magenta** to the maximum value displayed in **red**. The undefined values are displayed in **gray**, and denote the gridpoints at which at least one theoretical travel time is missing. The small cube has the sides of 2 km.

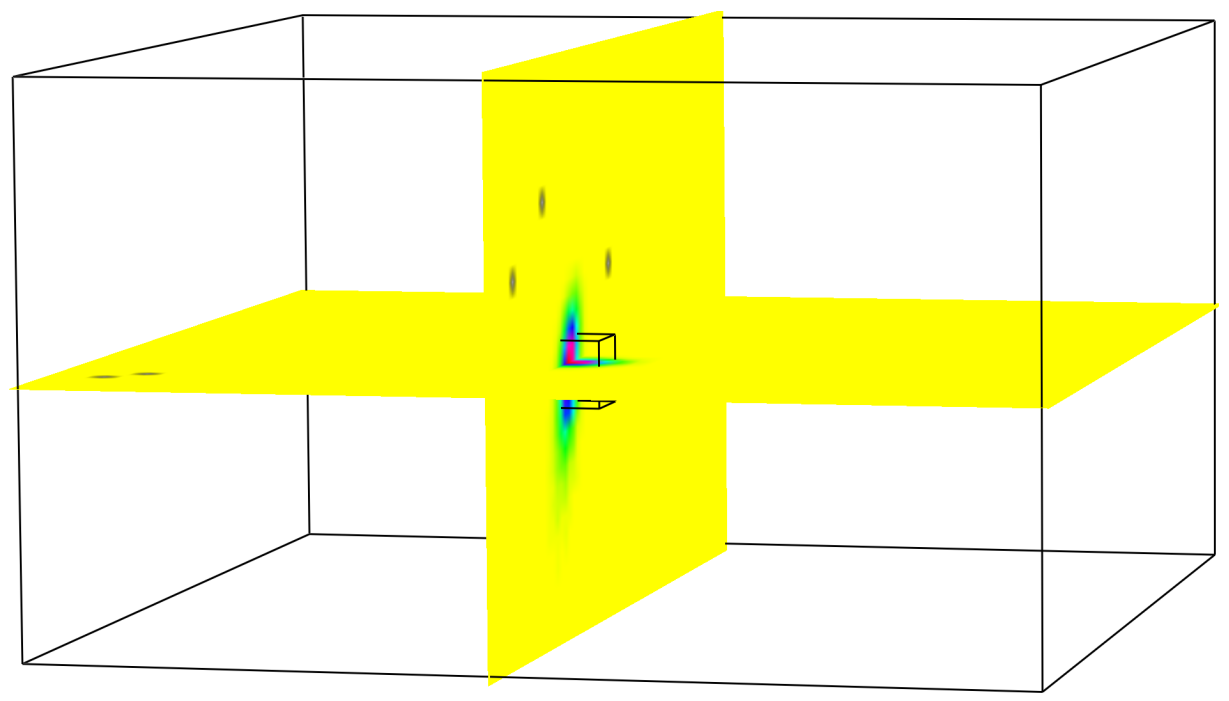

Nonnormalized 3–D marginal a posteriori density function of **event 3** determined using **10** P–wave arrival times. The zero values are displayed in **yellow**. The nonzero values range through **green**, **cyan**, **blue** and **magenta** to the maximum value displayed in **red**. The undefined values are displayed in **gray**, and denote the gridpoints at which at least one theoretical travel time is missing. The small cube has the sides of 2 km.

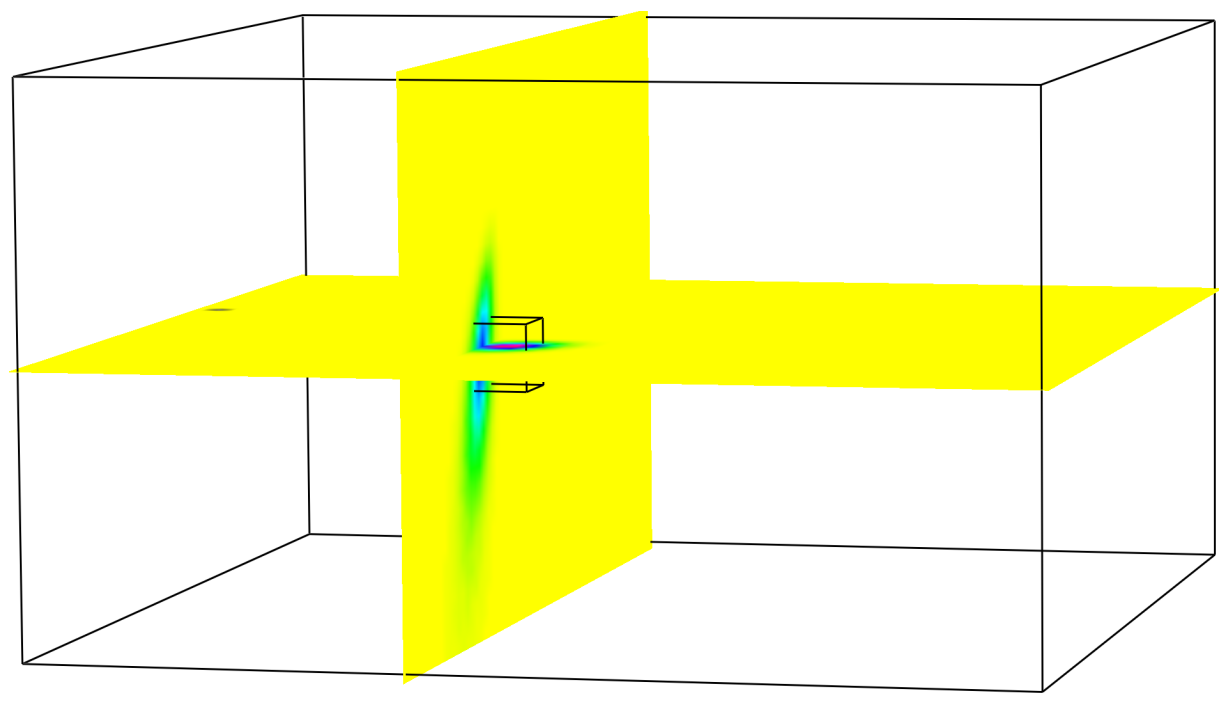

Nonnormalized 3–D marginal a posteriori density function of **event 4** determined using **6** P–wave arrival times. The zero values are displayed in **yellow**. The nonzero values range through **green**, **cyan**, **blue** and **magenta** to the maximum value displayed in **red**. The undefined values are displayed in **gray**, and denote the gridpoints at which at least one theoretical travel time is missing. The small cube has the sides of 2 km.

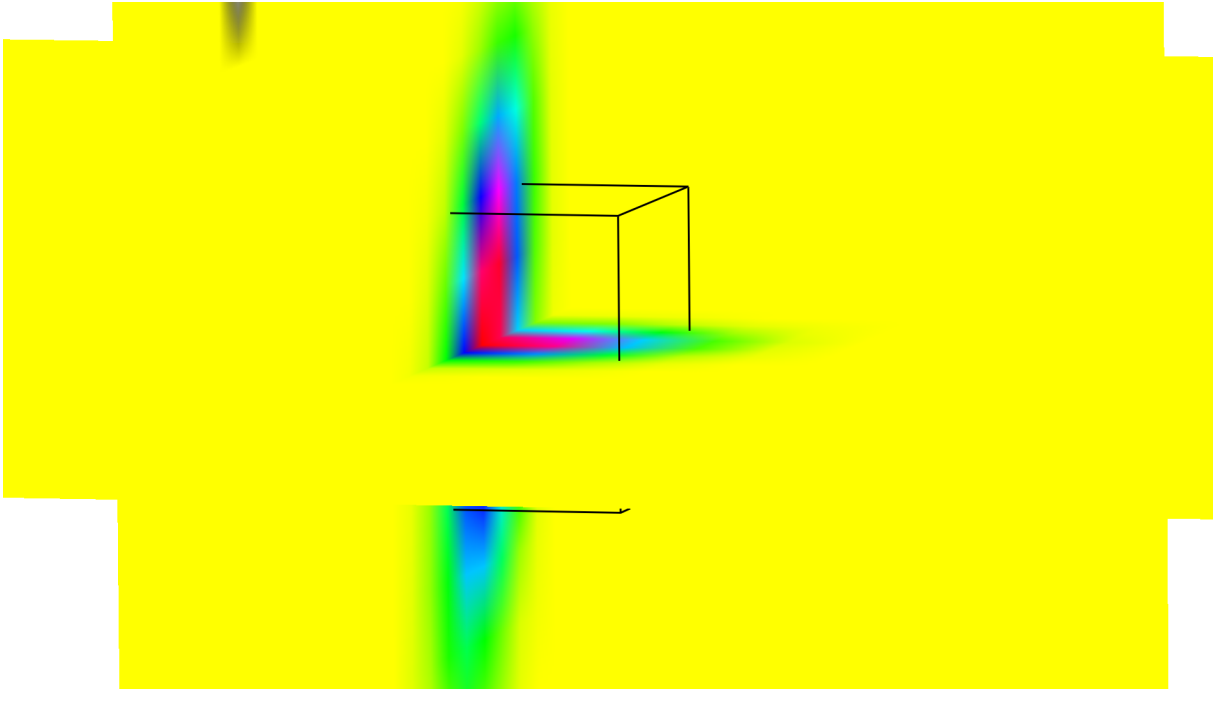

The detail of the interpolated discretized nonnormalized 3–D marginal a posteriori density function of **event 1**, displaying the hypocentral region. The cube has the sides of 2 km.

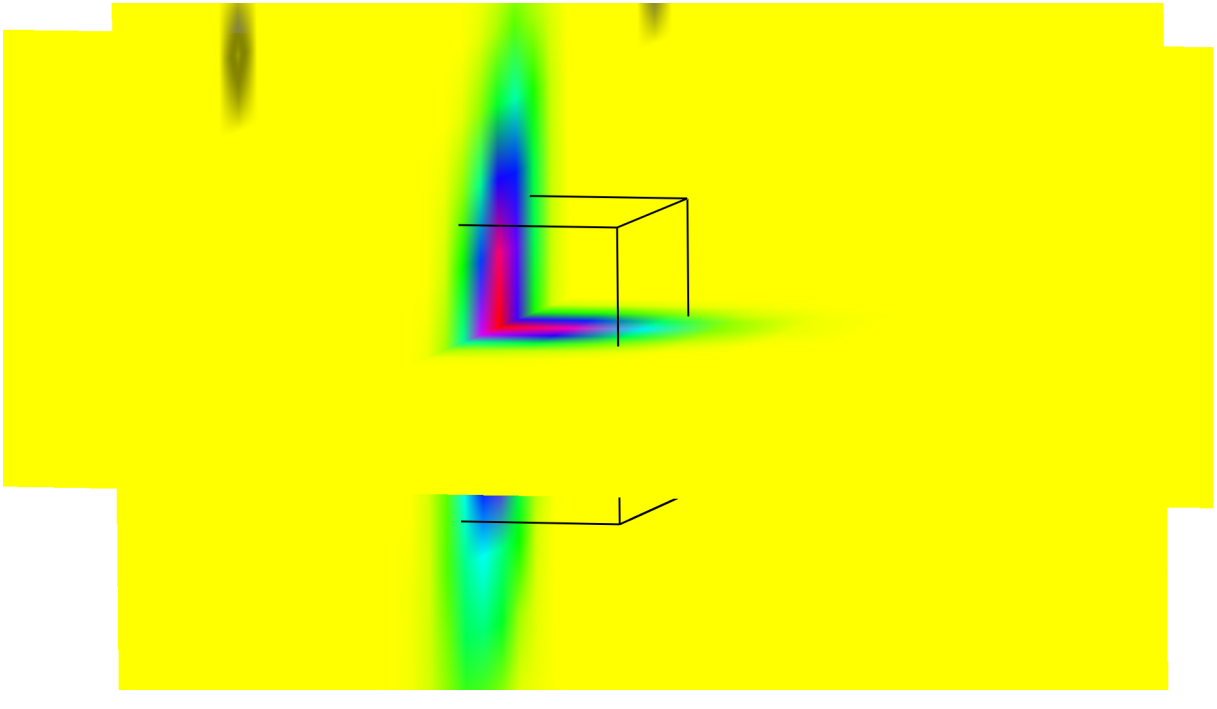

The detail of the interpolated discretized nonnormalized 3–D marginal a posteriori density function of **event 2**, displaying the hypocentral region. The cube has the sides of 2 km.

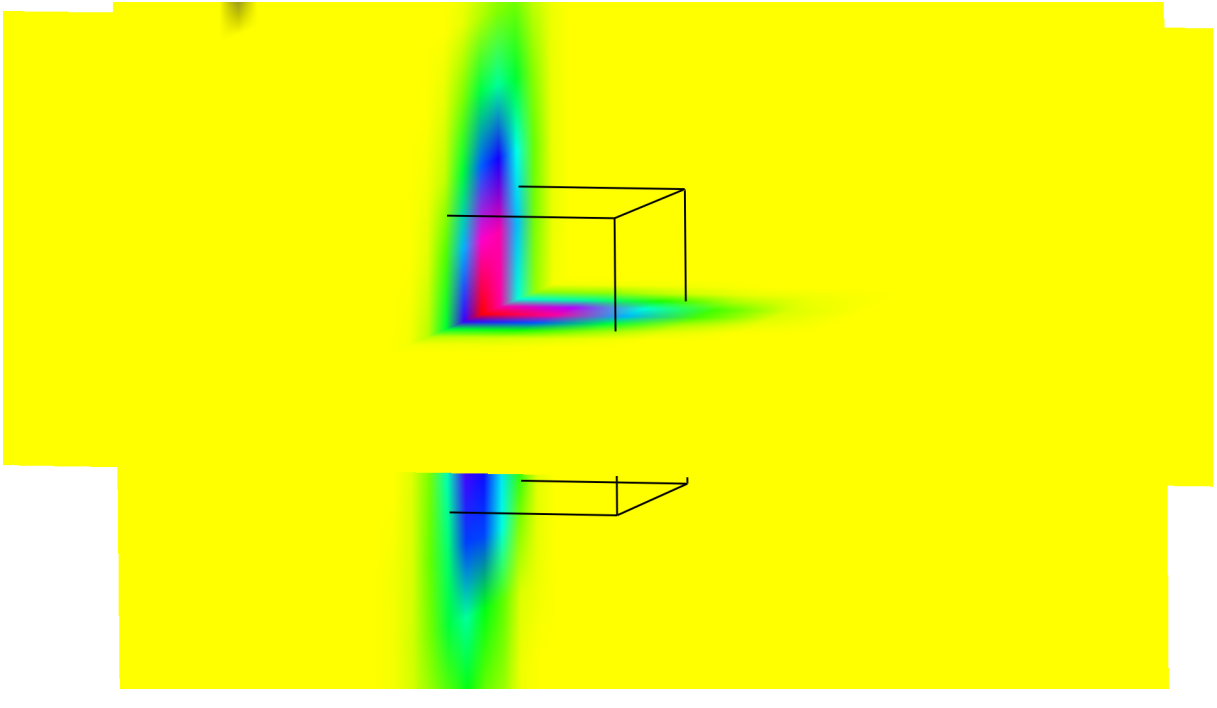

The detail of the interpolated discretized nonnormalized 3–D marginal a posteriori density function of **event 3**, displaying the hypocentral region. The cube has the sides of 2 km.

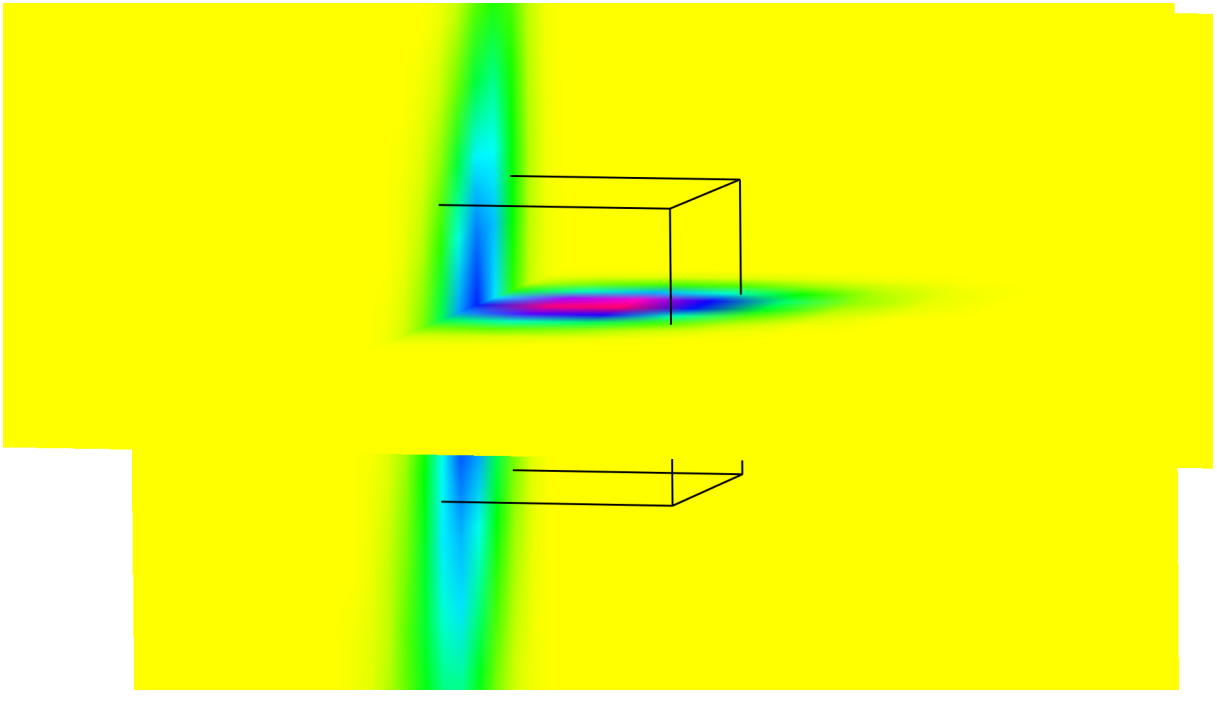

The detail of the interpolated discretized nonnormalized 3–D marginal a posteriori density function of **event 4**, displaying the hypocentral region. The cube has the sides of 2 km.

Numerical example 2

- microseismic monitoring of natural events, 33 events registered
- 15 stations, but each event was registered only on some of the stations (3 to 9 stations)
- simple 1-D layered velocity model consisting of 4 layers
- no information about the velocity model uncertainty

- we assumed power-law model covariance functions, used the value of Hurst exponent from Western Bohemia
- estimated separately P-wave and S-wave model inaccuracy, and then calculated the a posteriori density function using all the arrivals (as will be described on next two slides)

Numerical example 2

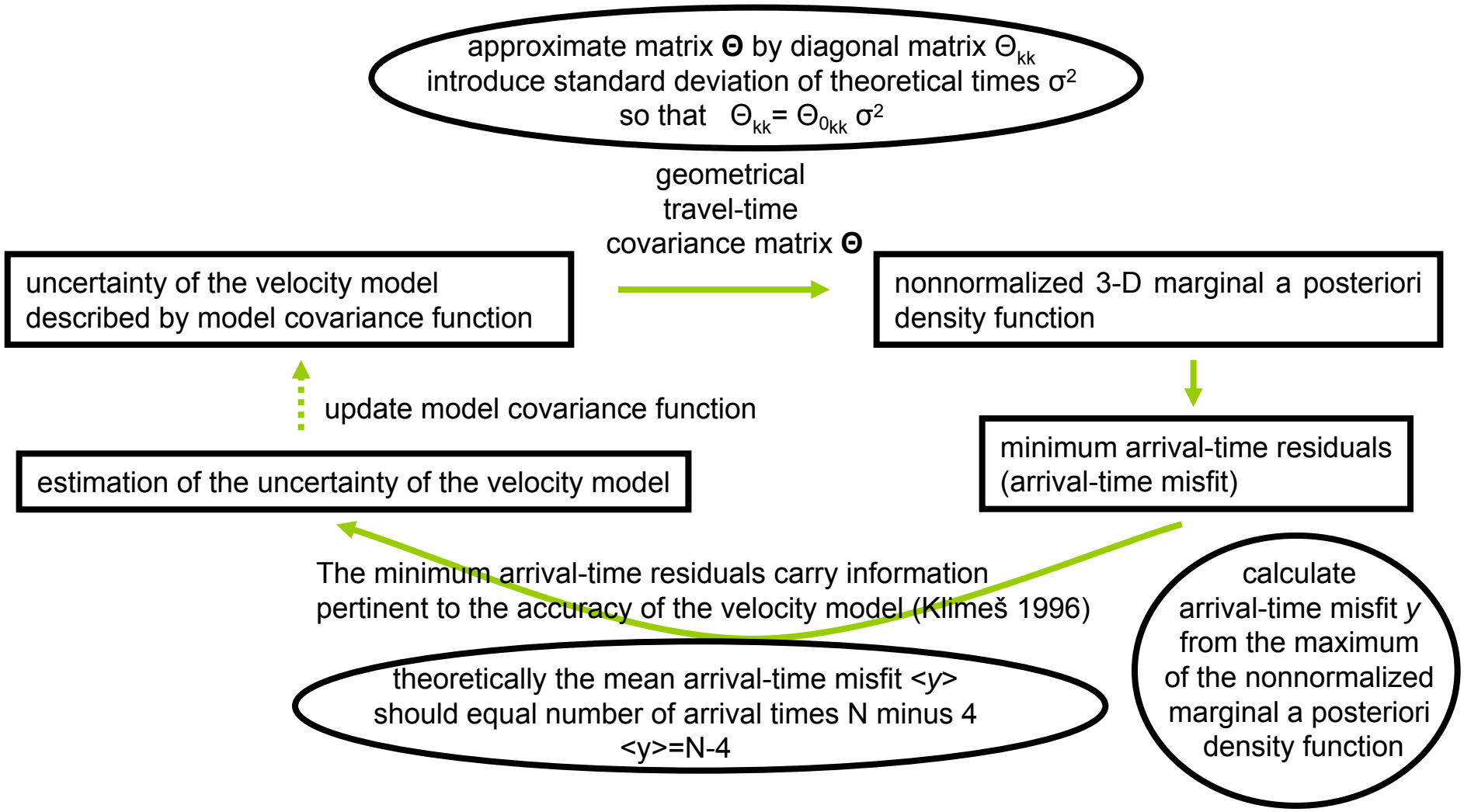

Numerical example 2

Iterative estimation of the model covariance function:

if we have sufficiently numerous set of events with sufficiently large numbers of arrivals:

step1:
- estimate uncertainty of the velocity model by choosing a value of σ
- calculate the a posteriori density function
- calculate arrival-time misfits *y* for all the events and calculate average $\underline{y}$
- compare with the average value of $\underline{N-4}$, update σ
- continue until we find σ for which $\underline{y} \sim \underline{N-4}$

Numerical example 2

Iterative estimation of the model covariance function:

if we have sufficiently numerous set of events with sufficiently large numbers of arrivals:

step1:
- estimate uncertainty of the velocity model by choosing a value of σ
- calculate the a posteriori density function
- calculate arrival-time misfits *y* for all the events and calculate average $\underline{y}$
- compare with the average value of $\underline{N-4}$, update σ
- continue until we find σ for which $\underline{y} \sim \underline{N-4}$

step 2:
- perform step 1 using P-wave arrivals to find σ_P
- perform step 1 using S-wave arrivals to find σ_S
- check whether the location with both P and S arrivals provides reasonable $\underline{y}_{S+P}$ so that $\underline{y}_{S+P} \sim \underline{N_S+N_P-4}$

Event	N_P	N_S	y_P	y_S	y_{P+S}
01	8	7	2.693	1.471	6.656
02	9	7	4.631	2.776	11.189
03	8	7	3.172	1.823	7.673
04	8	7	3.527	2.082	8.486
05	8	6	2.452	1.590	5.636
06	8	7	2.955	1.662	7.038
07	8	7	3.767	2.167	9.060
08	8	7	3.186	1.809	7.601
09	9	7	4.360	1.580	9.181
10	(5)	(5)			
11	8	7	3.000	2.969	8.833
12	(4)	(4)			
13	8	7	7.124	3.752	21.344
14	9	8	6.625	4.533	25.573
15	9	9	5.674	8.439	16.794
16	9	9	5.062	6.335	13.235
17	9	7	10.407	1.342	17.272
18	9	9	4.211	5.522	12.666
19	9	8	3.830	3.445	8.691
20	9	8	2.756	2.846	6.656
21	9	7	3.893	1.741	6.970
22	9	8	3.154	2.140	6.200
23	9	9	3.869	3.084	8.964
24	9	8	6.564	6.355	15.421
25	9	9	10.732	12.631	25.050
26	8	8	5.837	8.220	18.836
27	9	9	5.518	8.105	14.547
28	9	8	3.916	1.932	7.890
29	(5)	(3)			
30	8	8	3.675	4.818	12.946
31	8	7	3.591	3.988	11.129
32	8	6	5.314	1.011	7.535
33	7	7	1.869	3.084	7.751
Average	8.5	7.6	4.579	3.775	11.561

Numerical example 2 - results

- although we used the incorrect P-wave and S-wave geometrical travel time covariance matrices restricted just to diagonal elements, the behavior of the nonlinear hypocentre determination is reasonable – the average arrival-time misfit determined from both the P-wave and S-wave arrivals behaves in the same way it should behave for the correct geometrical travel-time covariance matrices

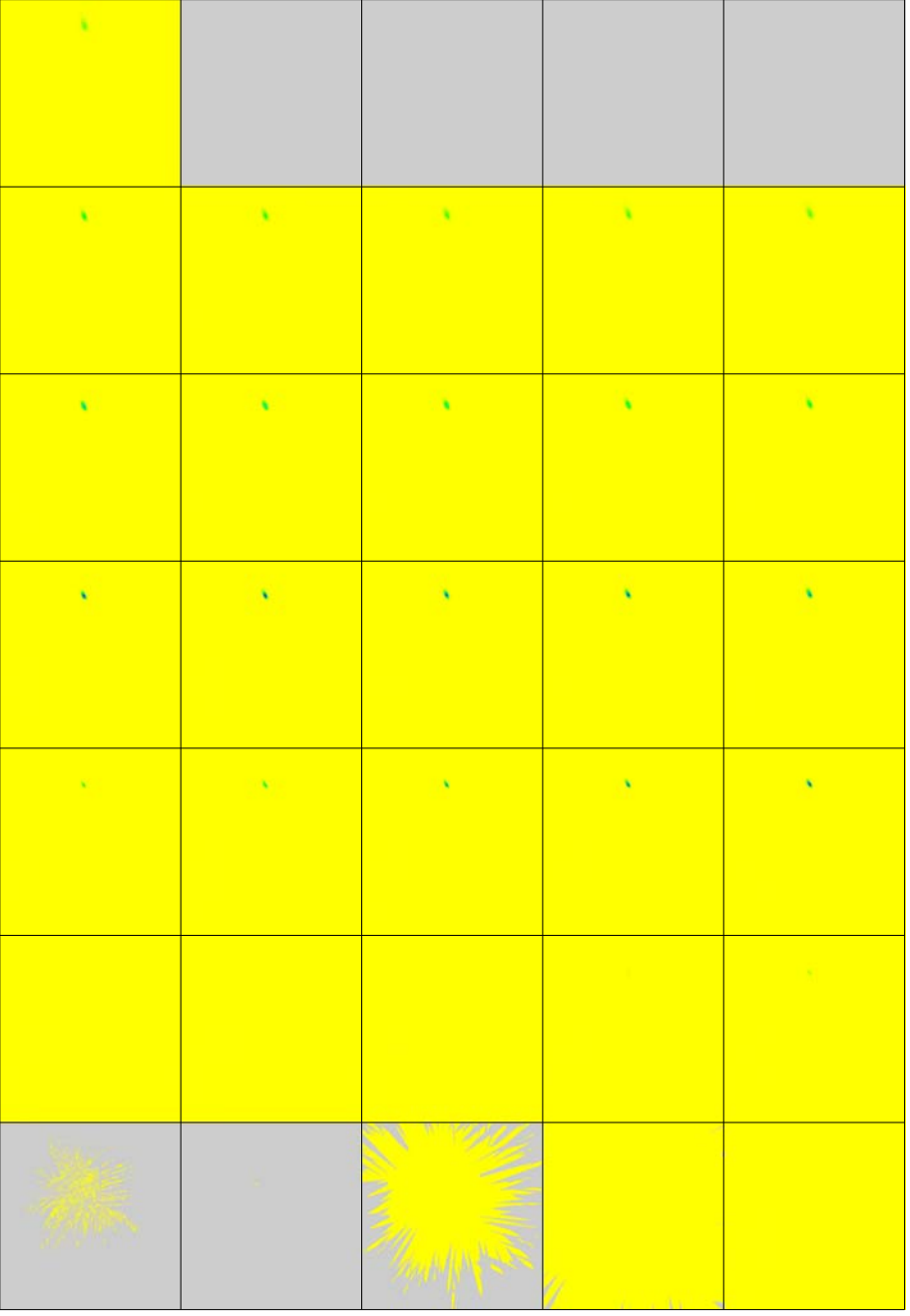

9 P-wave arrivals

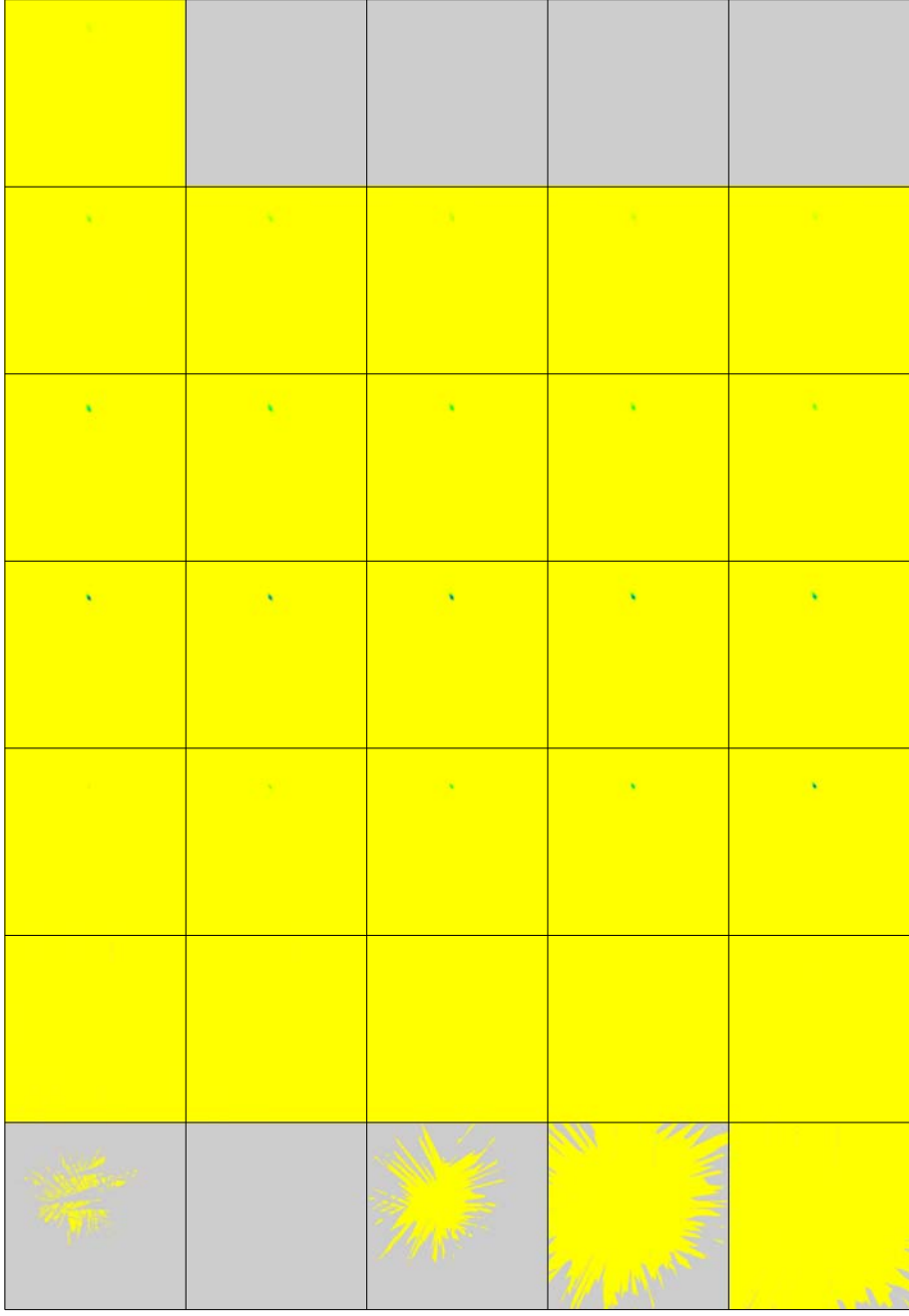

9 S-wave arrivals

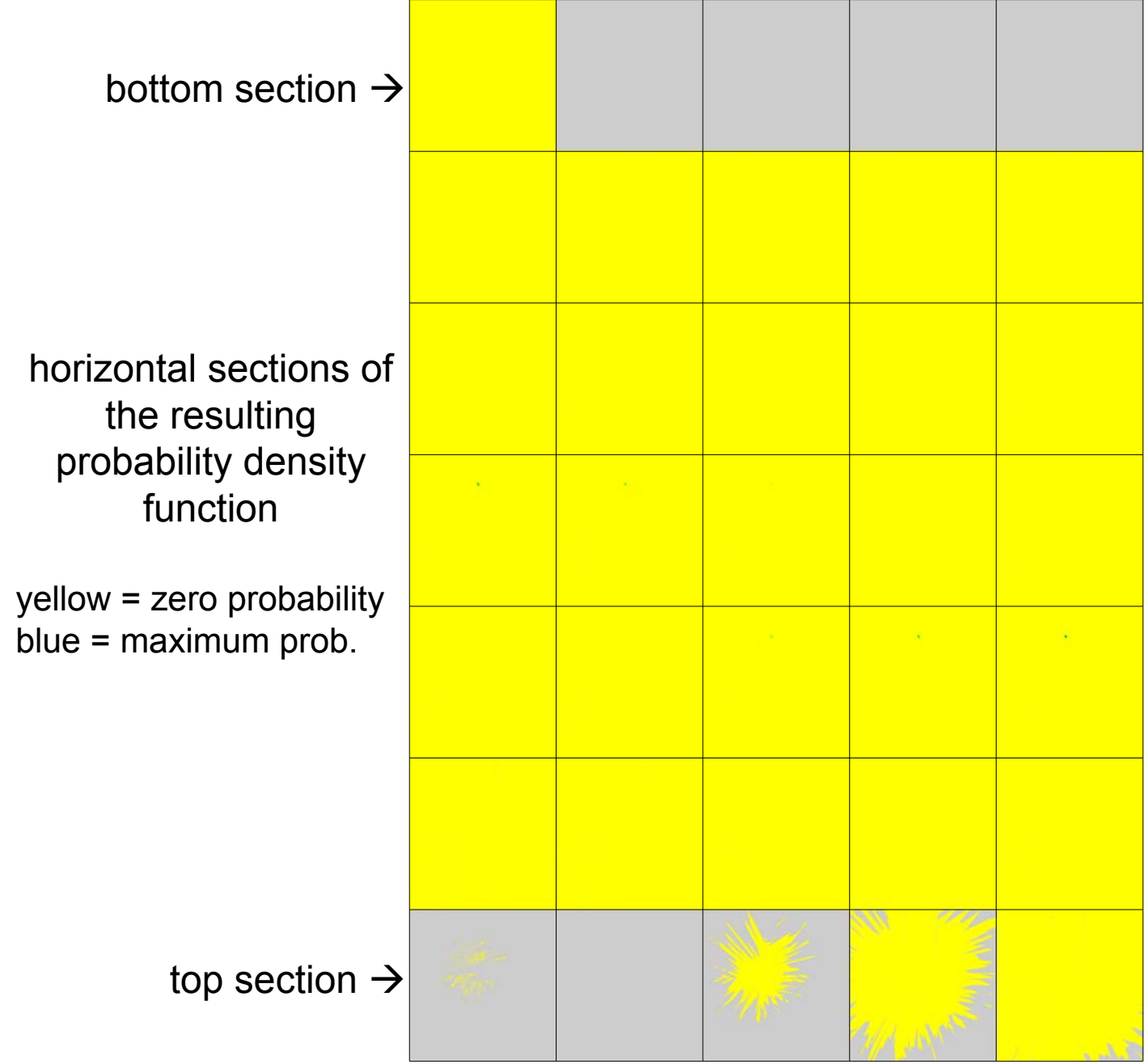
bottom section →
horizontal sections of the resulting probability density function
yellow = zero probability
blue = maximum prob.
top section →
9 P-wave arrivals + 9 S-wave arrivals

Numerical example 2 - results

- although we used the incorrect P-wave and S-wave geometrical travel time covariance matrices restricted just to diagonal elements, the behavior of the nonlinear hypocentre determination is reasonable – the average arrival-time misfit determined from both the P-wave and S-wave arrivals behaves in the same way it should behave for the correct geometrical travel-time covariance matrices

- when we use just P-wave or just S-wave arrival times, the depth of locations is uncertain for approximately 75% of events (including events with 9 arrivals)

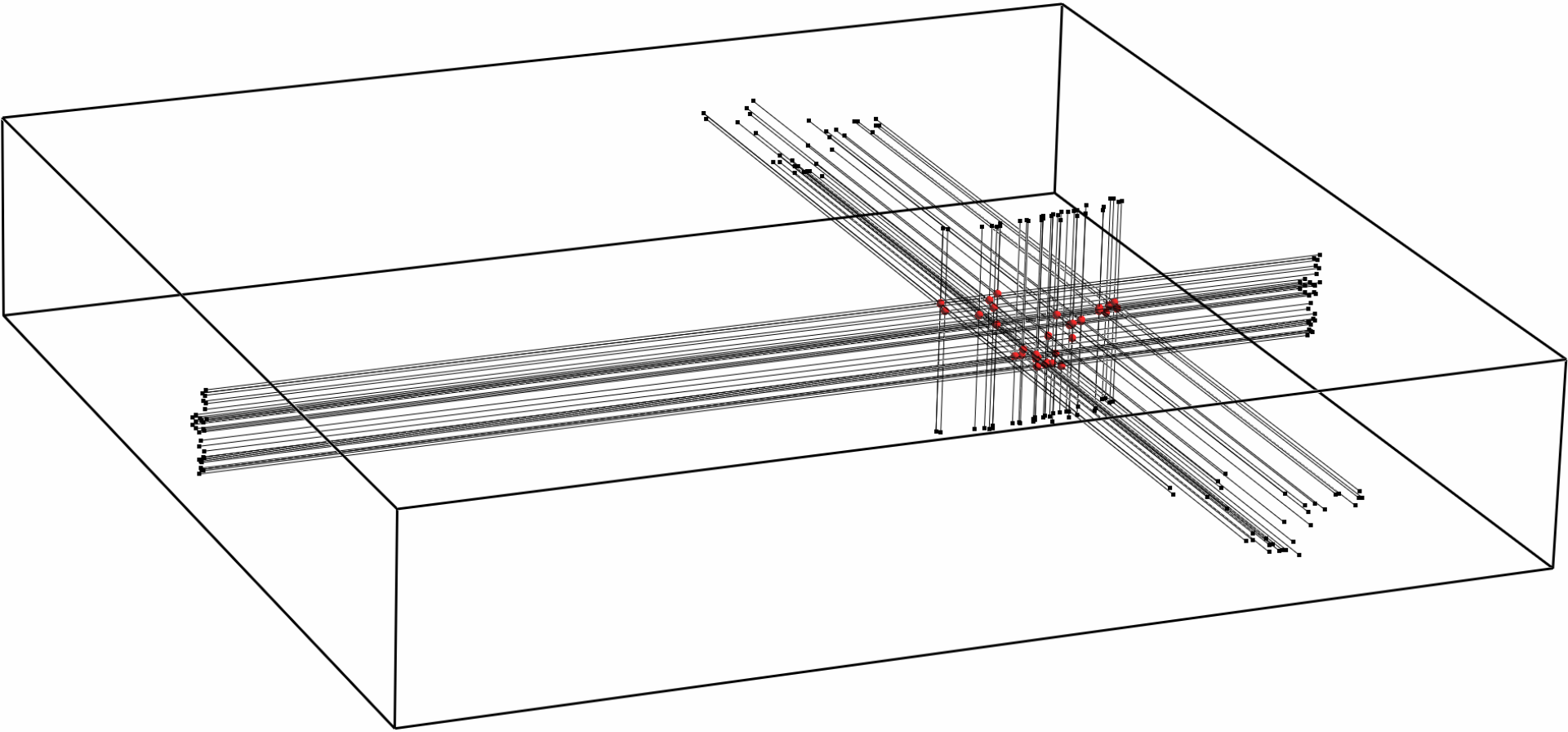

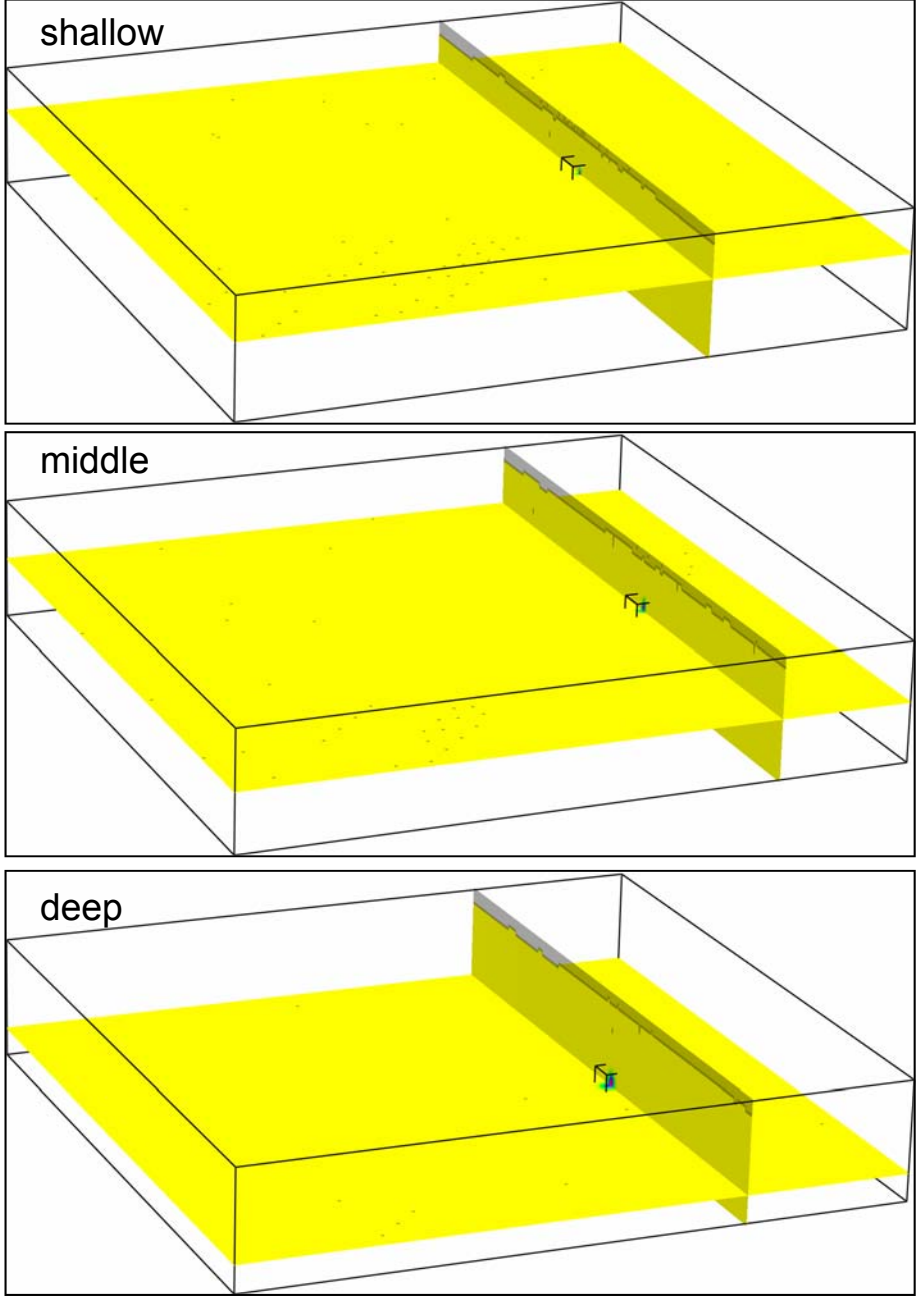

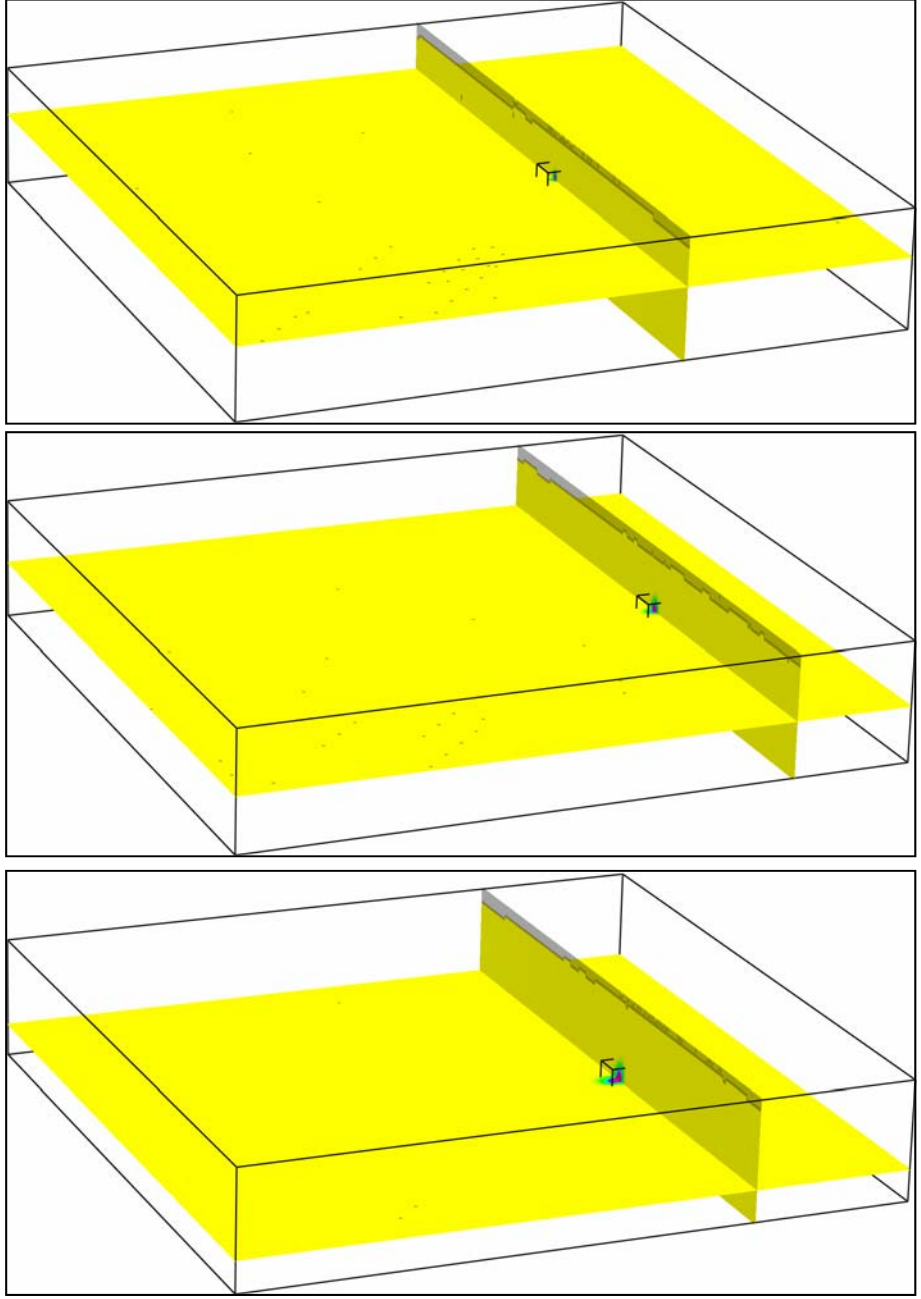

No. of arrivals: 9+9
9+9 (more arrivals)
9+7

8+6
8+7 (less arrivals)
4+4

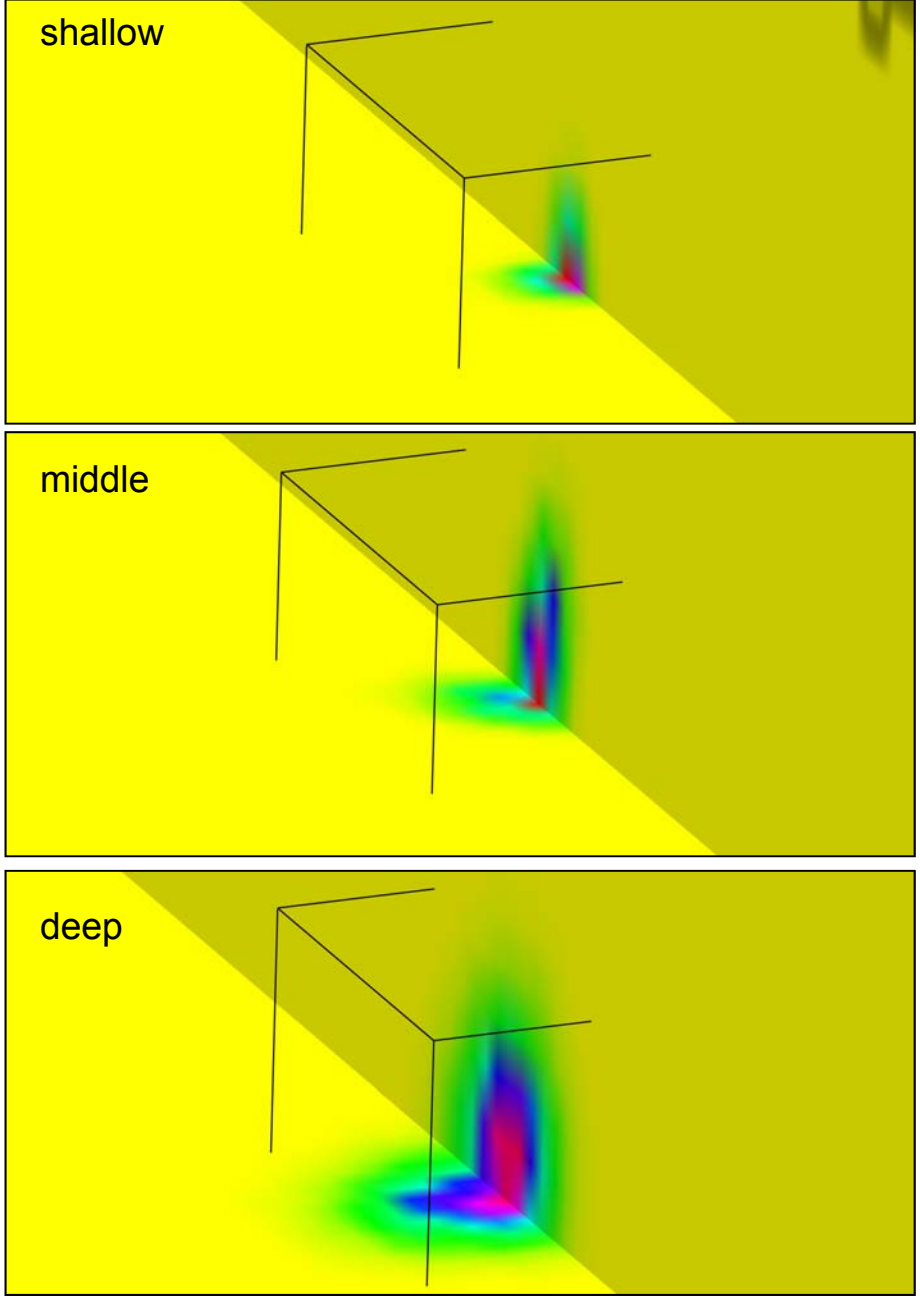

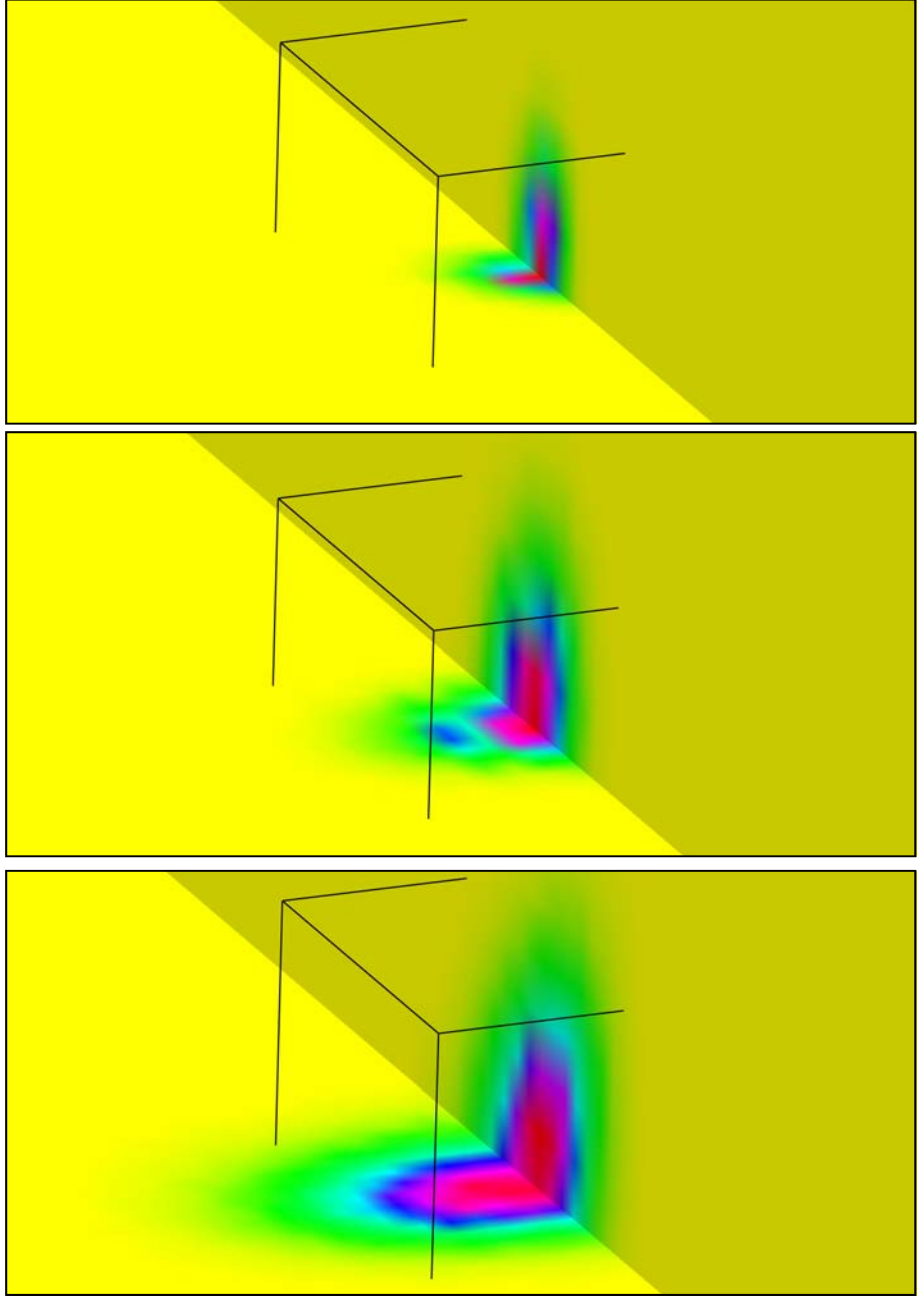

No. of arrivals: 9+9
9+9 (more arrivals)
9+7

8+6
8+7 (less arrivals)
4+4

Numerical example 2 - results

- although we used the incorrect P-wave and S-wave geometrical travel time covariance matrices restricted just to diagonal elements, the behavior of the nonlinear hypocentre determination is reasonable – the average arrival-time misfit determined from both the P-wave and S-wave arrivals behaves in the same way it should behave for the correct geometrical travel-time covariance matrices

- when we use just P-wave or just S-wave arrival times, the depth of locations is uncertain for approximately 75% of events (including events with 9 arrivals)

- when we use both P-wave and S-wave arrivals, we observe that the uncertainty of the hypocentral location increases with increasing depth and decreasing number of arrivals

Conclusions

We considered the robust nonlinear approach to hypocentre determination proposed by Tarantola & Valette (1982), consisting in direct evaluation of the nonnormalized 3–D marginal a posteriori density function which describes the relative probability of the seismic hypocentre, and proposed the corresponding numerical algorithm.

The nonnormalized 3–D marginal a posteriori density function allows for testing the model covariance function describing the uncertainty of the velocity model.

If we were able to use the whole geometrical travel-time covariance matrix, we could estimate the uncertainty of the velocity model.

Acknowledgments

The research has been supported by the Grant Agency of the Czech Republic under contract P210/10/0736, by the Ministry of Education of the Czech Republic within research projects MSM0021620860 and CzechGeo/EPOS LM2010008, and by the members of the consortium “Seismic Waves in Complex 3-D Structures".

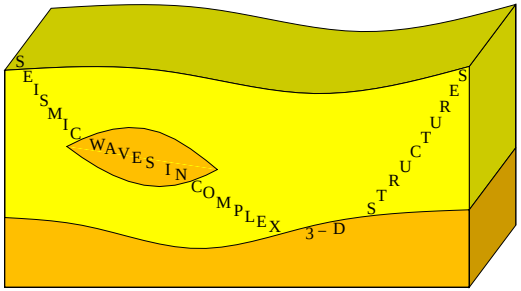

http://sw3d.cz

References

• Bucha, V. & Klimeš, L. (2015): Nonlinear hypocentre determination in the 3-D Western Bohemia a priori velocity model. *Seismic Waves in Complex 3-D Structures*, **25**, 37-50 , online at “http://sw3d.cz”.

• Bulant, P. & Klimeš, L. (2015): Nonlinear hypocentre determination. *Seismic Waves in Complex 3–D Structures*, **25**, 17–36, online at “http://sw3d.cz”.

• Klimeš, L. (1995): Examples of seismic models. *Seismic Waves in Complex 3–D Structures*, **3**, 5–35, online at “http://sw3d.cz”.

•Klimeš, L. (1996): Arrival–time residuals and hypocentre mislocation. *Pure appl. Geophys.*, **148**, 337–342, online at “http://sw3d.cz”.

• Klimeš, L. (2002a): Application of the medium covariance functions to travel–time tomography. *Pure appl. Geophys.*, **159**, 1791–1810, online at “http://sw3d.cz”.

• Klimeš, L. (2002b): Estimating the correlation function of a self–affine random medium. *Pure appl. Geophys.*, **159**, 1833–1853, online at “http://sw3d.cz”.

• Klimeš, L. (2008): Calculation of the a priori geometrical covariances of travel times in a self–affine random medium. *Seismic Waves in Complex 3–D Structures*, **18**, 27–70, online at “http://sw3d.cz”.

• Tarantola, A. & Valette, B. (1982): Inverse problems = quest for information. *J. Geophys.*, **50**, 159–170.